Jiao et al. Int J Concr Struct Mater (2019) 13:57
https://doi.org/10.1186/s40069-019-0362-z

International Journal of Concrete Structures and Materials

ORIGINAL ARTICLE

Open Access

A New 3D Empirical Plastic and Damage Model for Simulating the Failure of Concrete Structure

Yan-tao Jiao[1], Bo Wang[1*] and Zhen-zhong Shen[2]

Abstract

A new plastic–damage constitutive model based on the combination of damage mechanics and classical plastic theory was developed to simulate the failure of concrete. In order to explain different material behaviors of concrete under tensile and compressive loadings, the plastic yield criterion, the different kinematic hardening rule for tension and compressive and the isotropic flow rule were established in the effective stress space. Meanwhile, two different empirical damage evolution equations were adopted: one for compression and the other for tension. A multi-axial damage influence factor was also introduced to fully describe the anisotropic damage of concrete. Finally, the model response was compared with a wide range of experiment results. The results showed that the model could well describe the nonlinear behavior of concrete in a complex stress state.

Keywords: concrete, plastic–damage model, anisotropic damage, multi-axial damage influence factor, tensile damage, compressive damage

1 Introduction

This study mainly aimed to formulate a new plastic–damage constitutive model for concrete as completely and as simply as possible.

Existing plastic–damage models (PDMs) of concrete are usually based on sound thermodynamic principles (Hesebeck 2001; Mahnken 2002; Voyiadjis and Deliktas 2000; Cicekli et al. 2007; Taqieddin et al. 2012; Voyiadjis et al. 2008; Abu Al-Rub and Kim 2010; Wu et al. 2006; Liu et al. 2013; Mazars and Pijaudier-Cabot 1989; Lee and Fenves 1998). The thermodynamics-based damage model conforms to rigorous mechanical inference and has a solid theoretical foundation, therefore, it is called the theoretical plastic–damage model. Similar to the traditional plastic mechanics theory, a damage criteria and a damage dissipation potential function are needed to set up these models. However, it is hard to define the damage dissipation potential. In order to simplify the derivation of the model, some authors abandoned the thermodynamics-based damage criteria and turned to the empirically defined ones. One popular pattern of this kind of PDMs is that the models rely on the combination of stress-based plasticity formulated in the effective stress space with a strain-based damage model combined which can be obtained by empirical observations. These works (Grassl and Jir Sek 2006a, b; Grassl et al. 2013; Kitzig and Häußler-Combe 2011; Murakami 2012; Valentini and Hofstetter 2013) belong to this group. The models can be called the empirical plastic–damage models. As the damage model is based on strain, it may be easily implemented into commonly used strain-driven finite element procedures and the calculation of damage variable can be implemented explicitly. Thus, there are robust algorithms for FEM.

However, given the complex anisotropic damage in concrete, some authors adopted a single damage variable for both tension and compression (Grassl and Jir Sek 2006a, b; Yu et al. 2010; Kitzig and Häußler-Combe 2011; Valentini and Hofstetter 2013). This is sufficient for monotonic loading with unloading, but it is not suitable

*Correspondence: wangbo@ncwu.edu.cn
[1] School of Water Conservancy, North China University of Water Resources and Electric Power, Zhengzhou 450045, China
Full list of author information is available at the end of the article
Journal information: ISSN 1976-0485 / eISSN 2234-1315

for modeling the transition from tensile to compressive failure (i.e. the unilateral effect and elastic stiffness recovery under cyclic loading). In order to overcome this limitation, other authors adopted two isotropic damage variables: one for tension and the other for compression (Grassl et al. 2013; Murakami 2012). In spite of the satisfactory results obtained under the pure tension and pure compression stress states, the anisotropic damage of concrete and the interaction effect of damage in the orthogonal direction under multi-axial stress states were usually neglected in these models. But in fact, the stress-based damage evolution function can also be adopted to formulate the anisotropic constitutive models for quasi-brittle materials which are typical examples (see e.g. Faria et al. 1998; Berto et al. 2014). However, in some cases, although axial stress is compression, the corresponding axial strain may be tension or compression. Tensile strain may lead to tensile damage, and in this case, if the stress state is adopted to judge the damage state, the tensile damage may be ignored. Therefore, it is a controversial issue to define that the damage state is compression or tension through the stress state. Though it is also an open question to take strain as a state variable, strain is still used in many models. Moreover, as described by Challamel et al. (2005), damage is mainly a strain-controlled phenomenon. In this paper, we tended to use strain as a state variable to judge the damage state and to establish the damage evolution function.

With inspirations from all the previous works and understandings mentioned above, this paper presented a new PDM for concrete with two different empirical and strain-based damage evolution equations: one for tensile damage and the other for compressive damage. Under multi-axial stress states, the anisotropic damage and the interaction effect of damage in the orthogonal direction were considered and a multi-axial damage influence factor was introduced to extend the uniaxial damage evolution equation to a multi-axial form. As shown by Abu Al-Rub and Voyiadjis (2003), Cicekli et al. (2007) and Abu Al-Rub and Kim (2010), the plastic part of coupled plastic–damage model formulated in the effective space was numerically more stable and attractive. Thus in this paper, the plastic part of the proposed model was established in the effective stress space. Meanwhile, in order to simplify the derivation of constitutive equations and to bring advantages to the numerical implementation, the strain equivalence hypothesis was adopted in this paper. In addition, for the PDMs, the calibration of the material parameters usually relies on monotonic stress–strain experimental curves, but this results in a non-unique determination of the material parameters. Therefore, a simple and effective method which needs the uniaxial cyclic loading stress–strain experimental curves to identify the material parameters was proposed by Abu Al-Rub and Kim (2010). However, since the uniaxial cyclic tests are relatively complex, the stress–strain data is usually obtained by uniaxial monotonic test in actual engineering. Therefore, the method proposed by Abu Al-Rub and Kim (2010) to determine the material parameters may cause the lack of uniaxial cyclic loading stress–strain data. In order to overcome this limitation, a new method for the calibration of the material parameters was proposed in this paper.

Finally, a new empirical plastic and anisotropic damage model for plain concrete was formulated here. In the model, different responses of concrete under tension and compression were considered, including the effect of stiffness degradation, the interaction effects of damage in the orthogonal direction and the stiffness recovery due to crack closure in cyclic loading. To demonstrate the capability of the proposed model, the model response was compared with a wide range of experimental results.

2 Theoretical Basics of Plastic-Damage Model

2.1 Damage Part

2.1.1 Definition of Damage Variable

According to Rabotnov (1968), the relation between the nominal stress and the effective stress can be expressed as:

$$\bar{\sigma} = \frac{\sigma}{1-d} \tag{1}$$

where

$$d = \frac{A - \bar{A}}{A} = \frac{A^D}{A} \tag{2}$$

where A, A^D and $\bar{A}$ respectively denote the whole area, the total damage area and the effective area. d denotes the isotropic damage variable which varies from 0 to 1. The sign $(\overline{\bigcirc})$ denotes the physical quantity of the effective configuration corresponding to the nominal configuration $(\bigcirc)$.

Similarly, if the isotropic damage model is adopted under multi-axial stress state, the relation between the effective stress tensor $\bar{\boldsymbol{\sigma}}$ and the nominal stress tensor $\boldsymbol{\sigma}$ can be expressed as follows:

$$\bar{\boldsymbol{\sigma}} = (1-d)^{-1}\boldsymbol{\sigma} \tag{3}$$

By cutting out the section to determine the amount of holes, cracks and to accumulate the amount, the damage density of material can be directly determined, i.e. the damage variable d can be determined by Eq. (2). However, it is very difficult to put it into practice. In order to indirectly determine the damage density and simplify the derivation of constitutive equations, the strain equivalence hypothesis was proposed by Lemaitre and Chanboche (1974). Based on the strain equivalence hypothesis, the total nominal strain tensor $\boldsymbol{\varepsilon}$ can be set equal to the corresponding effective strain tensor $\bar{\boldsymbol{\varepsilon}}$, which can be decomposed into an elastic strain $\boldsymbol{\varepsilon}^{\mathrm{e}}(=\bar{\boldsymbol{\varepsilon}}^{\mathrm{e}})$ and a plastic strain $\boldsymbol{\varepsilon}^{\mathrm{p}}\ (=\bar{\boldsymbol{\varepsilon}}^{\mathrm{p}})$, such that:

$$\boldsymbol{\varepsilon}=\boldsymbol{\varepsilon}^{\mathrm{e}}+\boldsymbol{\varepsilon}^{\mathrm{p}}=\bar{\boldsymbol{\varepsilon}}^{\mathrm{e}}+\bar{\boldsymbol{\varepsilon}}^{\mathrm{p}}=\bar{\boldsymbol{\varepsilon}} \tag{4}$$

It should be noted that the original formulation of the strain equivalence hypothesis only applies to the elastic strain, i.e. one can only assume that the nominal elastic strain tensor $\boldsymbol{\varepsilon}^{\mathrm{e}}$ is equal to the corresponding effective elastic strain tensor $\bar{\boldsymbol{\varepsilon}}^{\mathrm{e}}$. However, as described by Abu Al-Rub and Voyiadjis (2003) and Cicekli et al. (2007), the additional permanent strain caused by damage in the nominal configuration was minimal and could be neglected. In this paper, the nominal plastic strain tensor $\boldsymbol{\varepsilon}^{p}$ was assumed to equal the corresponding effective plastic strain tensor $\bar{\boldsymbol{\varepsilon}}^{p}$. For simplicity, in this form, the strain equivalence hypothesis was used in these works, see e.g. Lee and Fenves (1998), Cicekli et al. (2007); Wu et al. (2006), Abu Al-Rub and Kim (2010), Liu et al. (2013), Grassl and Jir Sek (2006a), Grassl et al. (2013), Murakami (2012), Faria et al. (1998) and Al-Rub et al. (2013).

Based on Eqs. (3), (4) and the generalized Hook's law, the stress–strain relationship can be expressed as:

$$\begin{aligned}\boldsymbol{\sigma}&=\boldsymbol{E}:\boldsymbol{\varepsilon}^{\mathrm{e}}=\boldsymbol{E}:(\boldsymbol{\varepsilon}-\boldsymbol{\varepsilon}^{\mathrm{P}})=(1-d)\bar{\boldsymbol{E}}:(\boldsymbol{\varepsilon}-\boldsymbol{\varepsilon}^{\mathrm{P}})\\&=(1-d)\bar{\boldsymbol{E}}:\bar{\boldsymbol{\varepsilon}}^{\mathrm{e}}=(1-d)\bar{\boldsymbol{\sigma}}\end{aligned} \tag{5}$$

where $\boldsymbol{E}$ is the fourth-order damaged elastic stiffness tensor, which is a function of the damage variable d and $\overline{\boldsymbol{E}}$ is the fourth-order initial undamaged elastic stiffness tensor. For isotropic linear-elastic material, $\overline{\boldsymbol{E}}$is given by:

$$\overline{E}_{ijkl}=2\overline{G}\delta_{ik}\delta_{jl}+\left(\overline{K}-\frac{2}{3}\overline{G}\right)\delta_{ij}\delta_{kl} \tag{6}$$

where $\overline{G}=\bar{E}_0/2(1+\bar{\nu})$ and $\overline{K}=\bar{E}_0/3(1-2\bar{\nu})$ are respectively the effective shear and bulk moduli with $\bar{E}_0$ being the initial Young's modulus and $\bar{\nu}$ being the Poisson's ration.

Based on Eq. (5), the indirect form of damage variable expressed by stiffness degradation can be shown as follows:

$$d=1-\boldsymbol{E}:\bar{\boldsymbol{E}}^{-1} \tag{7}$$

For the case of one-dimension, the above equation can be rewritten as:

$$d=1-\frac{E}{\bar{E}_0} \tag{8}$$

where E is the damaged Young's modulus.

It is assumed in isotropic damage that the strength and stiffness of the concrete material are equally degraded in different directions upon damage evolution, but this is not the fact. In order to capture the load-induced anisotropy of concrete, the second-order symmetric damage tensor ω_{ij} was adopted in this paper. Matrix representation of the tensor ω_{ij} in the principal axes is as follows:

$$\left[\omega_{ij}\right]=\begin{bmatrix}\hat{\omega}_1 & & \\ & \hat{\omega}_2 & \\ & & \hat{\omega}_3\end{bmatrix} \tag{9}$$

where $\hat{\omega}_i,\ i=1,2,3$ represents the eigenvalues and can be expressed as:

$$\hat{\omega}_i=1-\frac{E_i}{\bar{E}_0},\ i=1,2,3 \tag{10}$$

In the subsequent development, the superscript hat symbol $(\hat{\bullet})$ denotes a principal value of $(\bullet)$.

E_i is an unknown quantity to be determined by the strain-based damage evolution function.

2.1.2 Damage Evolution Function

Since damage is an irreversible process, in this paper, the damage evolution function was described by the damage loading equations, loading–unloading conditions and the evolution laws for damage variables. In addition, given that the damage mechanisms of concrete behave differently in tension and compression, to better describe the different damage mechanisms under tensile and compressive loadings, two different empirical and strain-based damage evolution equations were adopted in this paper. Hereafter, the superscripts "+" and "−" respectively denote the tensile and compressive entities.

1. Uniaxial damage evolution function

The uniaxial damage (i.e. isotropic damage) loading functions and loading–unloading conditions can be expressed as:

$$f_d^{\pm}=\beta\hat{\varepsilon}^{\pm}(\hat{\bar{\sigma}}^{\pm})-k_d^{\pm} \tag{11}$$

$$k_d^{\pm}=\beta\hat{\varepsilon}^{\pm}(\hat{\bar{\sigma}}^{\pm}),\beta=\begin{cases}1 & if\ \hat{\varepsilon}^{+}\geq 0\\ -1 & if\ \hat{\varepsilon}^{-}<0\end{cases} \tag{12}$$

$$f_d^{\pm}\leq 0,\ \dot{k}_d^{\pm}\geq 0,\ \dot{k}_d^{\pm}f_d^{\pm}=0 \tag{13}$$

where $f_d^{\pm}$ is the axial loading function, $\hat{\varepsilon}^{\pm}(\hat{\bar{\sigma}}^{\pm})$ is the axial strain and $k_d^{\pm}$ is the axial damage-driven history variable which is used to store the maximum value that the axial strain can reach. Therefore, the axial damage-driven history variable $k_d^{\pm}$ never decreases even when the corresponding axial strain $\hat{\varepsilon}^{\pm}(\hat{\bar{\sigma}}^{\pm})$ decreases in the loading process.

The significance of damage loading functions and loading–unloading conditions can be simply interpreted as: if $f_d^{\pm} < 0$ and the material is in the cyclic loading or elastic unloading state, damage evolution cannot occur because the condition in Eq. (13) implies that $\dot{k}_d^{\pm} = 0$. If $f_d^{\pm} = 0$, the material can exhibit damage evolution characterized by $\dot{k}_d^{\pm} > 0$.

Since both damage and plastic deformations lead to the nonlinear response of concrete, both of the two deformations should be taken into account. For uniaxial tensile and compressive loading, $\hat{\bar{\sigma}}^+$ and $\hat{\bar{\sigma}}^-$ are given as (Lee and Fenves 1998)

$$\begin{aligned}\hat{\sigma}^+ &= (1-d^+)\hat{\bar{\sigma}}^+ = (1-d^+)\bar{E}_0\hat{\varepsilon}^{+e} \\ &= (1-d^+)\bar{E}_0(\hat{\varepsilon}^+ - \hat{\varepsilon}^{+p})\end{aligned} \tag{14}$$

$$\begin{aligned}\hat{\sigma}^- &= (1-d^-)\hat{\bar{\sigma}}^- = (1-d^-)\bar{E}_0\hat{\varepsilon}^{-e} \\ &= (1-d^-)\bar{E}_0(\hat{\varepsilon}^- - \hat{\varepsilon}^{-p})\end{aligned} \tag{15}$$

where $\hat{\varepsilon}^{\pm p}$ is the axial plastic strain which can be expressed by $\hat{\varepsilon}^{\pm p} = \int_0^t \dot{\hat{\varepsilon}}^{\pm p} dt$.

In this paper, the Guo-Zhang model recommended by code for design of concrete structure (GB50010-2002) (Ministry of Construction 2002) was adopted to express the stress–strain relation of concrete under the uniaxial stress state. For uniaxial tensile loading, the relation between stress and strain can be expressed as follows:

$$\begin{cases} \hat{\sigma}^+ = f_0^+\left(1.2\hat{x}^+ - 0.2\hat{x}^{+6}\right) & \text{if } \hat{x}^+ \le 1 \\ \hat{\sigma}^+ = f_0^+\hat{\mathrm{A}}^+ & \text{if } \hat{x}^+ > 1 \end{cases} \tag{16}$$

where $\hat{x}^+ = \hat{\varepsilon}^+/\varepsilon_0^+$, $\alpha_t = 0.312(f_0^+)^2$, f_0^+ is the uniaxial tensile strength and ε_0^+ is the strain corresponding to f_0^+. ε_0^+ and $\hat{\mathrm{A}}^+$ can be obtained by the following expression:

$$\begin{aligned}\varepsilon_0^+ &= \left(f_0^+\right)^{0.54} \times 65 \times 10^{-6}, \\ \hat{\mathrm{A}}^+ &= \hat{x}^+ / \left(\alpha_t\left(\hat{x}^+ - 1\right)^{1.7} + \hat{x}^+\right)\end{aligned} \tag{17}$$

where α_t is the material parameter and can be obtained by the following equation:

$$\alpha_t = 0.312(f_0^+)^2 \tag{18}$$

From Eq. (16), it is known that f_0^+ is a cut-off point and before the point, material is linear-elastic and after the point, material shows nonlinear feature, i.e. the material response seems to be weakened as the plastic strain increases because the elastic stiffness of the material is degraded due to damage evolution after the cut-off point (see Fig. 1a).

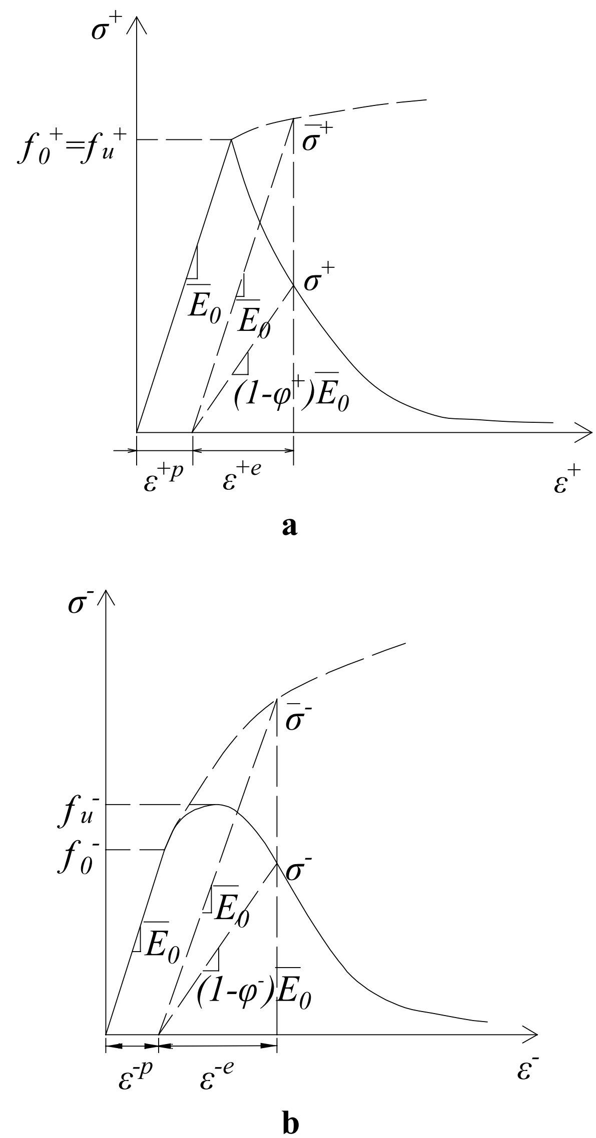

Fig. 1 Concrete behavior under uniaxial (**a**) tension and (**b**) compression.

Setting Eq. (14) equal to Eq. (16) and using k_d^+ to replace $\hat{\varepsilon}^+$ in Eqs. (14) and (16), the solving for d^+ will be:

$$d^+ = \begin{cases} 0 & \text{if } k_d^+ \le \varepsilon_0^+ \\ 1 - \frac{\varepsilon_0^+\hat{\mathrm{A}}^+}{(k_d^+ - \hat{\varepsilon}^{+p})} & \text{if } k_d^+ > \varepsilon_0^+ \end{cases} \tag{19}$$

For uniaxial compressive loading, the relation between stress and strain can be expressed as follows:

$$\begin{cases} \hat{\sigma}^- = \left(\bar{E}_0\varepsilon_u^-\right)\hat{x}^- & \text{if } \hat{x}^- \le 0.211 \\ \hat{\sigma}^- = f_u^-\hat{\mathrm{B}}^- & \text{if } 0.211 \le \hat{x}^- \le 1 \\ \hat{\sigma}^- = f_u^-\hat{C}^- & \text{if } \hat{x}^- > 1 \end{cases} \tag{20}$$

where $\hat{x}^- = \hat{\varepsilon}^-/\varepsilon_u^-$, f_u^- is the uniaxial compressive strength and ε_u^- is the strain corresponding to f_u^-. ε_u^-, $\hat{\mathrm{B}}^-$ and $\hat{C}^-$ can be expressed as:

$$\begin{aligned} \varepsilon_u^- &= \left(700 + 172\sqrt{f_u^-}\right) \times 10^{-6}, \\ \hat{\mathrm{B}}^- &= \alpha_a \hat{x}^- + (3 - 2\alpha_a)\hat{x}^{-2} + (\alpha_a - 2)\hat{x}^{-3}, \\ \hat{C}^- &= \hat{x}^-/\left(\alpha_d\left(\hat{x}^- - 1\right)^2 + \hat{x}^-\right) \end{aligned} \tag{21}$$

where α_a and α_d are the material parameters which can be obtained by the following equations:

$$\begin{aligned} \alpha_a &= 2.4 - 0.0125 f_u^-, \\ \alpha_d &= 0.157\left(f_u^-\right)^{0.785} - 0.905 \end{aligned} \tag{22}$$

From Fig. 1b, it can be seen that damage and plasticity are caused when the applied stress reaches $f_0^- = 0.4 f_u^-$ under uniaxial compressive loading. Therefore, using k_d^- to replace $\hat{\varepsilon}^-$ in Eq. (15), setting Eq. (15) equal to Eq. (20) and solving for d^-, the following can be obtained:

$$d^- = \begin{cases} 0 & \textit{if } 0 \le k_d^- < \left|0.211\varepsilon_u^-\right| \\ 1 - \frac{|f_u^-|\hat{\mathrm{B}}^-}{\bar{E}_0(k_d^- - |\hat{\varepsilon}^{-p}|)} & \textit{if } \left|0.211\varepsilon_u^-\right| \le k_d^- < \left|\varepsilon_u^-\right| \\ 1 - \frac{|f_u^-|\hat{C}^-}{\bar{E}_0(k_d^- - |\hat{\varepsilon}^{-p}|)} & \textit{if } \left|\varepsilon_u^-\right| \le k_d^- \end{cases} \tag{23}$$

where $|\bullet|$ is a symbol of absolute value.

2. Multi-axial damage evolution functiopn

Although uniaxial damage evolution law can reflect the general rule of damage evolution under uniaxial stress state, the mechanical characteristics and damage evolution of concrete are greatly different under multi-axial stress states. And for multi-axial stress states, a more advanced multi-axial damage evolution law is required.

A lot of uniaxial loading experiments of concrete show that the propagation direction of cracks is perpendicular to the stress direction under uniaxial tensile loading and cracks are parallel to the loading direction under compressive loading. Therefore, for uniaxial tensile loading, the damage evolution direction is consistent with the stress direction, which can be called "direct damage". But for uniaxial compressive loading, the damage evolution direction is vertical to the stress direction, which can be called "indirect damage". According to the experiment results of these works (Peng et al. 1997; Kupfer et al. 1969; Gao et al. 2001), the compressive strength of concrete in biaxial compressive states was significantly higher than the strength in uniaxial compressive state; under biaxial tensile–compressive states, the tensile strength of concrete in one direction obviously decreased with the increase of compressive stress (or strain) in the orthogonal direction, and the effect on the compressive strength in one direction due to the tensile stress (or strain) in the orthogonal direction was not very obvious. However, under biaxial tensile states, the variation of the tensile strength caused by tensile stress (or strain) in the orthogonal direction was very small. Based on these experiment results, it was assumed that: (1) compressive strain affected the tensile or compressive damage in the orthogonal direction; (2) tensile strain did not affect the damage in the orthogonal direction. According to this assumption, a multi-axial damage influence factor was introduced to extend the uniaxial damage evolution equation to a multi-axial form.

The multi-axial damage loading functions and loading–unloading conditions can be expressed as:

$$f_d^{(i)} = \beta_i \hat{\varepsilon}_i(\hat{\bar{\sigma}}_i) - k_d^{(i)} \tag{24}$$

$$k_d^{(i)} = \beta_i \hat{\varepsilon}_i(\hat{\bar{\sigma}}_i), \beta_i = \begin{cases} 1 & \text{if } \hat{\varepsilon}_i \ge 0 \\ -1 & \text{if } \hat{\varepsilon}_i < 0 \end{cases} \tag{25}$$

$$f_d^{(i)} \le 0, \dot{k}_d^{(i)} \ge 0, \dot{k}_d^{(i)} f_d^{(i)} = 0 \tag{26}$$

where $f_d^{(i)}$ is the axial loading function, $\hat{\varepsilon}_i(\hat{\bar{\sigma}}_i)$ is the axial strain, $k_d^{(i)}$ is the axial damage-driven history variable and $i = 1, 2, 3$.

As it is shown in Fig. 2, assuming that the total damage in direction 1 is made up of many micro circular crack areas $\tilde{A}_{1j}^D$, the total damage area in direction 1 can be expressed as:

$$\tilde{A}_1^D = \sum \tilde{A}_{1j}^D = A_1 - \bar{A}_1 \tag{27}$$

where A_1 is the whole cross-sectional area and $\bar{A}_1$ is the effective load-carrying area.

Based on Eq. (2), neglecting the effect of strain in the orthogonal direction, the damage variable in direction 1 can be expressed as $d_1 = \tilde{A}_1^D / A_1$.

According to the linear-elastic fracture mechanics theory, in an infinite medium, including elliptical microcracks, there will be shear stress at the crack tip under

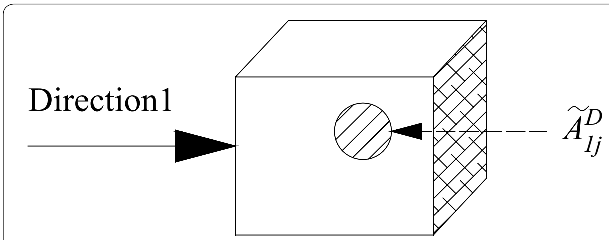

Fig. 2 Micro-defects of material in direction 1.

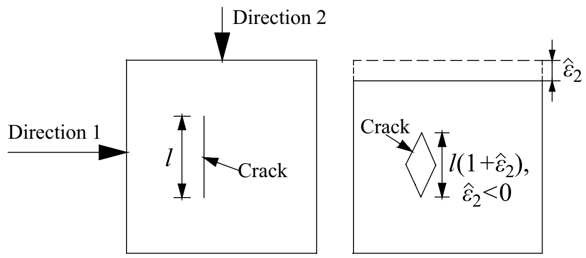

Fig. 3 Sketches of crack opening under compressive strain in direction 2.

uniaxial compressive loading and this will make the crack extend. It can be noted from Fig. 3 that if direction 1 is tensile strain and direction 2 is compressive strain (i.e. tension–compression combination), new crack extension will occur under the effect of compressive strain, and this will lead to the increase of the total damage area in direction 1 and will produce new damage. If setting the diameter of a damaged region $\tilde{A}_{1j}^D$ in direction 1 at loading step n as $l_{(n)}$ and the compressive strain in direction 2 as $\hat{\varepsilon}_{2(n)}$, with the effect of compressive strain $\hat{\varepsilon}_{2(n)}$ taken into account, the diameter of the damaged region $\tilde{A}_{1j}^D$ will reduce from $l_{(n)}$ to $l_{(n)}(1+\hat{\varepsilon}_{2(n)})$. Based on the geometrical relationship of Fig. 4a, the crack width $w_{(n)}$ can be expressed as follows:

$$w_{(n)} = \sqrt{-\hat{\varepsilon}_{2(n)}(2+\hat{\varepsilon}_{2(n)})}l_{(n)} \tag{28}$$

with $\hat{\varepsilon}_{2(n)} < 0$.

Furthermore, it can be noticed from Fig. 4a that w_c is a critical crack width. With the increase of the compressive strain $\hat{\varepsilon}_{2(n)}$, the diameter of the damaged region $\tilde{A}_{1j}^D$ will further decrease from $l_{(n)}(1+\hat{\varepsilon}_{2(n)})$ to $l_{(n)}(1+\hat{\varepsilon}_{2(n+1)})$. When the opening crack width $w_{(n)}$ reaches w_c, new crack propagation will occur. At this moment, it can be seen from Fig. 4b that the length of the crack will extend from $l_{(n)}(1+\hat{\varepsilon}_{2(n+1)})$ to $l'_{(n+1)}$. Based on the geometrical relationship of Fig. 4b, $w_{(n+1)}$ can be expressed as:

$$w_{(n+1)} = w_c = \sqrt{-\hat{\varepsilon}_{2(n+1)}(2+\hat{\varepsilon}_{2(n+1)})}l_{(n)} \tag{29}$$

with $\hat{\varepsilon}_{2(n+1)} < 0$.

And the extended area of the damage region $\tilde{A}_{1j}^D$ can be derived as:

$$A_{1j}^D = \tilde{A}_{1j}^D \frac{w_{(n+1)}^2\left(\hat{\varepsilon}_{2(n+1)}\right)}{w_{(n)}^2\left(\hat{\varepsilon}_{2(n)}\right)} \quad \left(\hat{\varepsilon}_{2(n+1)} < 0\right) \tag{30}$$

where A_{1j}^D is the extended area of the damage region $\tilde{A}_{1j}^D$.

Based on Eq. (30), the extended total damage area in direction 1 can be expressed as:

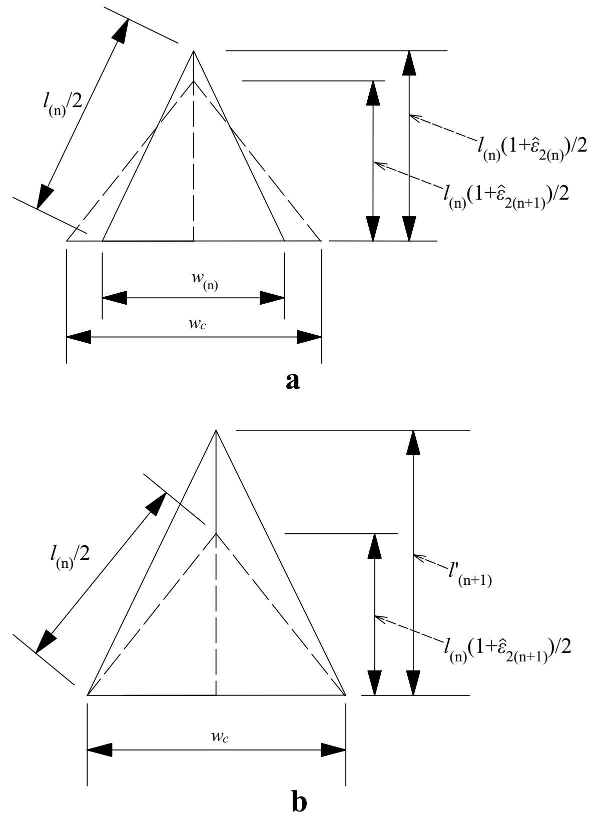

Fig. 4 The geometrical relationship between crack width and length. **a** Before crack propagation and **b** after crack propagation.

$$\begin{aligned} A_1^D &= \sum A_{1j}^D = \frac{w_{(n+1)}^2\left(\hat{\varepsilon}_{2(n+1)}\right)}{w_{(n)}^2\left(\hat{\varepsilon}_{2(n)}\right)} \sum \tilde{A}_{1j}^D \\ &= \frac{w_{(n+1)}^2\left(\hat{\varepsilon}_{2(n+1)}\right)}{w_{(n)}^2\left(\hat{\varepsilon}_{2(n)}\right)} \tilde{A}_1^D \quad \left(\hat{\varepsilon}_{2(n+1)} < 0\right) \end{aligned} \tag{31}$$

where A_1^D is the total damage area in direction 1 when the effect of $\hat{\varepsilon}_2$ is considered and $\tilde{A}_1^D$ is the total damage area in direction 1 when the effect of $\hat{\varepsilon}_2$ is neglected.

According to the above definition of damage variable and with the effect of compressive strain $\hat{\varepsilon}_2$ considered, the new damage $\hat{\omega}_1$ in direction 1 at step $n+1$ can be derived as:

$$\begin{aligned} \hat{\omega}_{1(n+1)} &= \frac{A_1^D}{A_1} = d_{1(n+1)}\left(\hat{\varepsilon}_{1(n+1)}\right) \frac{w_{(n+1)}^2\left(\hat{\varepsilon}_{2(n+1)}\right)}{w_{(n)}^2\left(\hat{\varepsilon}_{2(n)}\right)} \\ &= d_{1(n+1)}\left(\hat{\varepsilon}_{1(n+1)}\right) \chi_{2(n+1)} \quad \left(\hat{\varepsilon}_{2(n+1)} < 0\right) \end{aligned} \tag{32}$$

where $d_{1(n+1)}\left(\hat{\varepsilon}_{1(n+1)}\right)$ is the damage in direction 1 at step $n+1$ without considering the effect of $\hat{\varepsilon}_2$ and $\chi_{2(n+1)}$ is the tensile damage influence factor caused by compressive strain in direction 2 at step $n+1$.

Similarly, if direction 3 is also compressive strain, the damage in direction 1 can be written as follows:

$$\begin{aligned}\hat{\omega}_{1(n+1)} &= d_{1(n+1)}\left(\hat{\varepsilon}_{1(n+1)}\right)\chi_{2(n+1)}\,\chi_{3(n+1)} \\ &\times\left(\hat{\varepsilon}_{2(n+1)} < 0, \hat{\varepsilon}_{3(n+1)} < 0\right)\end{aligned} \tag{33}$$

As mentioned earlier, it is difficult to determine the damage variable by Eq. (2) (i.e. $d_i = (A_i - \bar{A}_i)/A_i (i = 1, 2, 3)$), thus, to determine the damage density indirectly, the strain equivalence hypothesis was proposed by Lemaitre and Chanboche (1974). This means that Eq. (2) is equivalent to Eq. (8), such that:

$$d_i = \frac{A_i - \bar{A}_i}{A_i} = \frac{\tilde{A}_i^D}{A_i} = 1 - \frac{E_i}{\bar{E}_0} \tag{34}$$

It should be noted that the uniaxial tensile damage evolution equation (19) is derived on the basis of the strain equivalence hypothesis (i.e. $d = 1 - E/\bar{E}_0$). Based on Eqs. (33, 19) can be extended to a multi-axial form as follows:

$$\hat{\omega}_i^+ = \begin{cases} 0 & \textit{if } k_d^{+(i)} \le \varepsilon_0^+ \\ \left[1 - \frac{\varepsilon_0^+ \hat{A}_i^+}{(k_d^{+(i)} - \hat{\varepsilon}_i^{+p})}\right] \prod\limits_{j=1}^{3} \chi_j & \textit{if } k_d^{+(i)} > \varepsilon_0^+ \end{cases} \tag{35}$$

with $i, j = 1, 2, 3$, and χ_j can be expressed as:

$$\chi_j = \frac{-\left(\hat{\varepsilon}_j + \Delta\hat{\varepsilon}_j\right)\left(2 + \hat{\varepsilon}_j + \Delta\hat{\varepsilon}_j\right)}{-\hat{\varepsilon}_j\left(2 + \hat{\varepsilon}_j\right)} \quad \left(\hat{\varepsilon}_j < 0\right). \tag{36}$$

When both direction 1 and direction 2 are compressive strain, the area of damage region in direction 1 will show a shrinking tendency due to the effect of compressive strain in direction 2, and the damage density in direction 1 will decrease. Therefore, a multi-axial compressive damage influence factor $\chi_i^{'}$ for compression-compression combination should be defined. Since the reduction of the damage density in direction 1 caused by the compressive strain in direction 2 was not very obvious, after repeated trials, the multi-axial compressive damage influence factor $\chi_i^{'}$ was assumed as a constant and 0.8 was used in the study. Substituting $\chi_i^{'}$ into Eq. (23), the multi-axial compressive damage evolution equation is shown as follows:

$$\hat{\omega}_i^- = \begin{cases} 0 & \textit{if } 0 \le k_d^{-(i)} < \left|0.211\varepsilon_u^-\right| \\ \left[1 - \frac{|f_u^-|\hat{B}_i^-}{\bar{E}_0\left(k_d^{-(i)} - \left|\hat{\varepsilon}_i^{-p}\right|\right)}\right] \prod\limits_{j=1}^{3} \frac{\chi_j^{'}}{\chi_i^{'}} & \textit{if } \left|0.211\varepsilon_u^-\right| \le k_d^{-(i)} < \left|\varepsilon_u^-\right| \\ \left[1 - \frac{|f_u^-|\hat{C}_i^-}{\bar{E}_0\left(k_d^{-(i)} - \left|\hat{\varepsilon}_i^{-p}\right|\right)}\right] \prod\limits_{j=1}^{3} \frac{\chi_j^{'}}{\chi_i^{'}} & \textit{if } \left|\varepsilon_u^-\right| \le k_d^{-(i)} \end{cases} \tag{37}$$

with $i, j = 1, 2, 3$.

2.1.3 Stiffness Degradation

1. Definition of Damaged Elastic Stiffness with Cyclic Loading Neglected

The degradation of stiffness caused by damage occurs in both tension and compression and becomes more significant as the strain increases. Since the anisotropic damage tensor was adopted in this paper, Eq. (3) can be extended as:

$$\bar{\boldsymbol{\sigma}} = (\boldsymbol{I} - \boldsymbol{\omega})^{-1}\boldsymbol{\sigma}. \tag{38}$$

As described by Murakami (2012), the effective stress tensor obtained by Eq. (38) was asymmetric. Since it is usually inconvenient to use the asymmetric effective stress tensor in the formulation of constitutive and evolution equations, several symmetrization methods were proposed by many authors. The method proposed by Cordebois and Sidoroff (1982) is used frequently (Carol et al. 2001; Prochtel and Häußler-Combe 2008; Mozaffari and Voyiadjis 2015; Murakami 2012). By this method, Eq. (38) can be rewritten as follows:

$$\bar{\boldsymbol{\sigma}} = (\boldsymbol{I} - \boldsymbol{\omega})^{-1/2}\boldsymbol{\sigma}(\boldsymbol{I} - \boldsymbol{\omega})^{-1/2} \tag{39}$$

or

$$\boldsymbol{\sigma} = \boldsymbol{M}(\boldsymbol{\omega}) : \bar{\boldsymbol{\sigma}} \tag{40}$$

where

$$\begin{aligned} M_{ijkl} = \frac{1}{2}\Big[&(\delta_{ik} - \omega_{ik})^{1/2}(\delta_{jl} - \omega_{jl})^{1/2} \\ &+ (\delta_{il} - \omega_{il})^{1/2}(\delta_{jk} - \omega_{jk})^{1/2}\Big]. \end{aligned} \tag{41}$$

In the principal coordinate system of damage $\boldsymbol{\omega}$ with the Voigt notations, the fourth-order damage-effect tensor $\boldsymbol{M}$ can be expressed as the following "diagonal matrix form":

$$\left[\boldsymbol{M}(\hat{\boldsymbol{\omega}})\right] = dig\left[\,\phi_1 \;\; \phi_2 \;\; \phi_3 \;\; \sqrt{\phi_2\phi_3} \;\; \sqrt{\phi_1\phi_3} \;\; \sqrt{\phi_1\phi_2}\,\right] \tag{42}$$

where $\phi_i = 1 - \hat{\omega}_i$ with $\hat{\omega}_i (i = 1, 2, 3)$ being the principal damage variable.

As described by Chow and Wang (1987), since the fourth-order damage-effect tensor M_{ijkl} contained more individual components and the elements in a fourth-order tensor were difficult if not impossible to be measured, the simplification became necessary for practical reasons. Zhu and Cescotto (1995), Chow and Wang (1987) and Zhang et al. (2001) used the simplified damage effect tensor in Eq. (42) to establish the relation between the effective and nominal stress tensors, and the matrix representation of the nominal stress tensor can be written as:

$$\{\sigma\} = [E]\{\varepsilon - \varepsilon^p\} = [E]\{\varepsilon^e\} \tag{43}$$

where

$$\begin{aligned} \{\sigma\} &= \begin{bmatrix} \sigma_{11} & \sigma_{22} & \sigma_{33} & \sigma_{23} & \sigma_{13} & \sigma_{12} \end{bmatrix}^T \\ \{\varepsilon\} &= \begin{bmatrix} \varepsilon_{11} & \varepsilon_{22} & \varepsilon_{33} & \varepsilon_{23} & \varepsilon_{13} & \varepsilon_{12} \end{bmatrix}^T \end{aligned} \tag{44}$$

and

$$[E] = \varpi \cdot \begin{bmatrix} E_1(1-\bar{\nu}) & E_1\bar{\nu} & E_1\bar{\nu} & 0 & 0 & 0 \\ E_2\bar{\nu} & E_2(1-\bar{\nu}) & E_2\bar{\nu} & 0 & 0 & 0 \\ E_3\bar{\nu} & E_3\bar{\nu} & E_3(1-\bar{\nu}) & 0 & 0 & 0 \\ 0 & 0 & 0 & \frac{E_{23}(1-2\bar{\nu})}{2} & 0 & 0 \\ 0 & 0 & 0 & 0 & \frac{E_{13}(1-2\bar{\nu})}{2} & 0 \\ 0 & 0 & 0 & 0 & 0 & \frac{E_{12}(1-2\bar{\nu})}{2} \end{bmatrix} \tag{45}$$

with $E_i = \phi_i \bar{E}_0$, $E_{ij} = \sqrt{\phi_i\phi_j}\bar{E}_0 (i,j = 1,2,3)$ and $\varpi = 1/(1+\bar{\nu})(1-2\bar{\nu})$.

Combining Eqs. (14), (15) and (43)–(45), it can be seen that the principal nominal stress can be expressed as:

$$\hat{\sigma}_i = \phi_i\left(\bar{K} + \frac{4}{3}\bar{G}\right)\hat{\varepsilon}_i^e + \phi_i\left(\bar{K} - \frac{2}{3}\bar{G}\right)\sum_{j=1}^{3}\hat{\varepsilon}_j^e. \tag{46}$$

When a single damage variable for both tension and compression is adopted, the pattern of stiffness degradation defined in Eq. (45) will be applicable, e.g. Kitzig and Häußler-Combe (2011). However, if two different damage variables for tension and compression are adopted, in some cases, it may be inappropriate to establish the constitutive relationship. Taking the true tri-axial compressive test reported by Van Mier (1984) as an example, when the stress ratio was $\hat{\sigma}_1/\hat{\sigma}_2/\hat{\sigma}_3 = -1/-0.1/-0.05$, only $\hat{\varepsilon}_1$ was compressive strain and both $\hat{\varepsilon}_2$ and $\hat{\varepsilon}_3$ were tensile strains. In this case, the negative and positive principal nominal stress components were $\hat{\boldsymbol{\sigma}}^- = \left(\hat{\sigma}_1^-, 0.1\hat{\sigma}_1^-, 0.05\hat{\sigma}_1^-\right)^T$ and $\hat{\boldsymbol{\sigma}}^+ = (0,0,0)^T$. And the corresponding negative and positive principal strain components can be written as $\hat{\boldsymbol{\varepsilon}}^- = \left(\hat{\varepsilon}_1^-, 0, 0\right)^T$ and $\hat{\boldsymbol{\varepsilon}}^+ = \left(0, \hat{\varepsilon}_2^+, \hat{\varepsilon}_3^+\right)^T$. By using the damaged elastic stiffness tensor defined in Eq. (45), the principal nominal stress vector can be expressed as:

$$\begin{Bmatrix} \hat{\sigma}_1 \\ \hat{\sigma}_2 \\ \hat{\sigma}_3 \end{Bmatrix} = \begin{bmatrix} \phi_1(\hat{\varepsilon}_1) & & \\ & \phi_2(\hat{\varepsilon}_2) & \\ & & \phi_3(\hat{\varepsilon}_3) \end{bmatrix} \begin{Bmatrix} \hat{\bar{\sigma}}_1 \\ \hat{\bar{\sigma}}_2 \\ \hat{\bar{\sigma}}_3 \end{Bmatrix}. \tag{47}$$

Obviously, when a single damage variable for both tension and compression is adopted, the above equation is reasonable. But when two different damage variables are adopted, Eq. (47) can be rewritten as:

$$\begin{Bmatrix} \hat{\sigma}_1^- \\ \hat{\sigma}_2^- \\ \hat{\sigma}_3^- \end{Bmatrix} = \begin{bmatrix} \phi_1^-(\hat{\varepsilon}_1^-) & & \\ & \phi_2^+(\hat{\varepsilon}_2^+) & \\ & & \phi_3^+(\hat{\varepsilon}_3^+) \end{bmatrix} \begin{Bmatrix} \hat{\bar{\sigma}}_1^- \\ \hat{\bar{\sigma}}_2^- \\ \hat{\bar{\sigma}}_3^- \end{Bmatrix}. \tag{48}$$

It can be seen that the mixing term $\phi^+(\hat{\varepsilon}^+) \cdot \hat{\bar{\sigma}}^-$ in Eq. (48) is in conflict with Eqs. (14), (15) and it cannot reflect the different damage mechanisms under tensile and compressive loadings. In order to eliminate the mixing term and to include the unilateral effect, the spectral decomposition technique can be used to separate the stress or strain tensor into positive and negative components. If the spectral decomposition of the stress tensor is performed, based on the assumption that the expression in Eq. (40) is valid for both tension and compression, such that:

$$\boldsymbol{\sigma}^+ = M^+(\omega^+) : \bar{\boldsymbol{\sigma}}^+, \quad \boldsymbol{\sigma}^- = M^-(\omega^-) : \bar{\boldsymbol{\sigma}}^-. \tag{49}$$

Then the total nominal stress tensor can be expressed as:

$$\boldsymbol{\sigma} = M^+(\omega^+) : \bar{\boldsymbol{\sigma}}^+ + M^-(\omega^-) : \bar{\boldsymbol{\sigma}}^-. \tag{50}$$

And Eq. (47) can be rewritten as:

$$\begin{aligned} \begin{Bmatrix} \hat{\sigma}_1 \\ \hat{\sigma}_2 \\ \hat{\sigma}_3 \end{Bmatrix} &= \begin{bmatrix} 1 & 0 & 0 \\ 0 & \phi_2^+(\hat{\varepsilon}_2^+) & 0 \\ 0 & 0 & \phi_3^+(\hat{\varepsilon}_3^+) \end{bmatrix} \begin{Bmatrix} 0 \\ 0 \\ 0 \end{Bmatrix} \\ &+ \begin{bmatrix} \phi_1^-(\hat{\varepsilon}_1^-) & 0 & 0 \\ 0 & 1 & 0 \\ 0 & 0 & 1 \end{bmatrix} \begin{Bmatrix} \hat{\bar{\sigma}}_1^- \\ \hat{\bar{\sigma}}_2^- \\ \hat{\bar{\sigma}}_3^- \end{Bmatrix} \end{aligned}. \tag{51}$$

From the above equation, it can be seen that the mixing term is eliminated, but a new issue is introduced (i.e. $\hat{\sigma}_2 = \hat{\bar{\sigma}}_2^-$ and $\hat{\sigma}_3 = \hat{\bar{\sigma}}_3^-$). Obviously, due to the characteristics of the damage evolution equations defined in this paper, the spectral decomposition of the stress tensor is unsuitable for this study. Therefore, the strain tensor will be separated into positive and negative components in the paper. By using the spectral decomposition technique, the following relation can be obtained:

$$\varepsilon_{ij}^+ = P_{ijkl}^+ \varepsilon_{kl}, \quad \varepsilon_{ij}^- = (I_{ijkl} - P_{ijkl}^+)\varepsilon_{kl} = P_{ijkl}^- \varepsilon_{kl} \tag{52}$$

where $I_{ijkl} = P_{ijkl}^+ + P_{ijkl}^-$ is the fourth identity tensor and

$$P_{ijkl}^+ = \sum_{k=1}^{3} H(\hat{\varepsilon}^{(k)}) n_i^{(k)} n_j^{(k)} n_k^{(k)} n_l^{(k)} \tag{53}$$

where $H(x)$ is the Heaviside step function ($H(x) = 1$ for $x > 0$ and $H(x) = 0$ for $x < 0$), $\hat{\varepsilon}^{(k)}$ is the kth principal strain of $\boldsymbol{\varepsilon}$ and $n_i^{(k)}$ is the kth corresponding unit principal direction.

Since the normalized eigenvector of the elastic tensor is identical to the normalized eigenvector of the total strain tensor, the positive and negative parts of the elastic strain tensor can be expressed as:

$$\begin{cases} \boldsymbol{\varepsilon}^{+e} = \boldsymbol{P}^+ : \boldsymbol{\varepsilon}^e = \boldsymbol{P}^+ : \left(\boldsymbol{\varepsilon} - \boldsymbol{\varepsilon}^p\right) \\ \boldsymbol{\varepsilon}^{-e} = \boldsymbol{P}^- : \boldsymbol{\varepsilon}^e = \boldsymbol{P}^- : \left(\boldsymbol{\varepsilon} - \boldsymbol{\varepsilon}^p\right) \end{cases}. \tag{54}$$

Therefore, the elastic strain tensor can be expressed as:

$$\begin{aligned} \boldsymbol{\varepsilon}^e &= \boldsymbol{I} : \boldsymbol{\varepsilon}^e = \left(\boldsymbol{P}^+ + \boldsymbol{I} - \boldsymbol{P}^+\right) : \boldsymbol{\varepsilon}^e \\ &= \boldsymbol{P}^+ : \boldsymbol{\varepsilon}^e + \boldsymbol{P}^- : \boldsymbol{\varepsilon}^e = \boldsymbol{\varepsilon}^{+e} + \boldsymbol{\varepsilon}^{-e} \end{aligned}. \tag{55}$$

Based on Eqs. (5) and (54), the positive and negative effective stress tensors can be expressed as follows:

$$\begin{cases} \bar{\boldsymbol{\sigma}}^+ = \bar{\boldsymbol{E}} : \boldsymbol{P}^+ : (\boldsymbol{\varepsilon} - \boldsymbol{\varepsilon}^p) = \bar{\boldsymbol{E}} : \boldsymbol{\varepsilon}^{+e} \\ \bar{\boldsymbol{\sigma}}^- = \bar{\boldsymbol{E}} : \boldsymbol{P}^- : (\boldsymbol{\varepsilon} - \boldsymbol{\varepsilon}^p) = \bar{\boldsymbol{E}} : \boldsymbol{\varepsilon}^{-e} \end{cases} \tag{56}$$

Based on Eq. (40), it is shown that $\boldsymbol{E} = \boldsymbol{M} : \bar{\boldsymbol{E}}$. Since $\boldsymbol{M}$ is a function of $\boldsymbol{\varepsilon}$, the positive and negative nominal stress tensors can be expressed as follows:

$$\begin{cases} \boldsymbol{\sigma}^+ = \boldsymbol{M}^+\left(\boldsymbol{\varepsilon}^+\right) : \bar{\boldsymbol{\sigma}}^+ = \boldsymbol{M}^+\left(\boldsymbol{\varepsilon}^+\right) : \bar{\boldsymbol{E}} : \boldsymbol{\varepsilon}^{+e} \\ = \boldsymbol{E}^+\left(\boldsymbol{\varepsilon}^+\right) : \boldsymbol{\varepsilon}^{+e} = \boldsymbol{E}^+\left(\boldsymbol{\varepsilon}^+\right) : \boldsymbol{P}^+ : (\boldsymbol{\varepsilon} - \boldsymbol{\varepsilon}^p) \\ \boldsymbol{\sigma}^- = \boldsymbol{M}^-\left(\boldsymbol{\varepsilon}^-\right) : \bar{\boldsymbol{\sigma}}^- = \boldsymbol{M}^-\left(\boldsymbol{\varepsilon}^-\right) : \bar{\boldsymbol{E}} : \boldsymbol{\varepsilon}^{-e} \\ = \boldsymbol{E}^-\left(\boldsymbol{\varepsilon}^-\right) : \boldsymbol{\varepsilon}^{-e} = \boldsymbol{E}^-\left(\boldsymbol{\varepsilon}^-\right) : \boldsymbol{P}^- : (\boldsymbol{\varepsilon} - \boldsymbol{\varepsilon}^p) \end{cases}. \tag{57}$$

Then, the nominal stress tensor can be expressed as:

$$\boldsymbol{\sigma} = \boldsymbol{\sigma}^+ + \boldsymbol{\sigma}^- = \boldsymbol{E}^+\left(\boldsymbol{\varepsilon}^+\right) : \boldsymbol{\varepsilon}^{+e} + \boldsymbol{E}^-\left(\boldsymbol{\varepsilon}^-\right) : \boldsymbol{\varepsilon}^{-e}. \tag{58}$$

In order to make it easy to write program, the above equation in matrix form can be written as:

$$\{\sigma\} = \left[E^+\left(\varepsilon^+\right)\right]\left\{\varepsilon^{+e}\right\} + \left[E^-\left(\varepsilon^-\right)\right]\left\{\varepsilon^{-e}\right\}. \tag{59}$$

with $\left[E^\pm\left(\varepsilon^\pm\right)\right]$ being the positive and negative damaged elastic stiffness matrixes which can be obtained by Eq. (45).

By the above method, Eq. (47) can be then rewritten as:

$$\begin{Bmatrix} \hat{\sigma}_1 \\ \hat{\sigma}_2 \\ \hat{\sigma}_3 \end{Bmatrix} = \varpi \bar{E}_0 (\Upsilon + \Psi). \tag{60}$$

with Υ being expressed as:

$$\Upsilon = \begin{bmatrix} (1-\bar{\nu}) & \bar{\nu} & \bar{\nu} \\ \phi_2^+ \bar{\nu} & \phi_2^+(1-\bar{\nu}) & \phi_2^+ \bar{\nu} \\ \phi_3^+ \bar{\nu} & \phi_3^+ \bar{\nu} & \phi_3^+(1-\bar{\nu}) \end{bmatrix} \begin{Bmatrix} 0 \\ \hat{\varepsilon}_2^+ \\ \hat{\varepsilon}_3^+ \end{Bmatrix}. \tag{61}$$

and Ψ being expressed as:

$$\Psi = \begin{bmatrix} \phi_1^-(1-\bar{\nu}) & \phi_1^- \bar{\nu} & \phi_1^- \bar{\nu} \\ \bar{\nu} & (1-\bar{\nu}) & \bar{\nu} \\ \bar{\nu} & \bar{\nu} & (1-\bar{\nu}) \end{bmatrix} \begin{Bmatrix} \hat{\varepsilon}_1^- \\ 0 \\ 0 \end{Bmatrix}. \tag{62}$$

By rearranging the above three equations, the following equation can be obtained:

$$\begin{Bmatrix} \hat{\sigma}_1 \\ \hat{\sigma}_2 \\ \hat{\sigma}_3 \end{Bmatrix} = \begin{bmatrix} 1 & 0 & 0 \\ 0 & \phi_2^+ & 0 \\ 0 & 0 & \phi_3^+ \end{bmatrix} \begin{Bmatrix} \hat{\bar{\sigma}}_1^+ \\ \hat{\bar{\sigma}}_2^+ \\ \hat{\bar{\sigma}}_3^+ \end{Bmatrix} + \begin{bmatrix} \phi_1^- & 0 & 0 \\ 0 & 1 & 0 \\ 0 & 0 & 1 \end{bmatrix} \begin{Bmatrix} \hat{\bar{\sigma}}_1^- \\ \hat{\bar{\sigma}}_2^- \\ \hat{\bar{\sigma}}_3^- \end{Bmatrix}. \tag{63}$$

From Eq. (63), it can be seen that when using the pattern of stiffness degradation defined in Eq. (45) and combining the spectral decomposition of the strain tensor to establish the constitutive relationship, although the result was improved, there were still some issues, i.e. the effective stress components $\hat{\bar{\sigma}}_1^+$, $\hat{\bar{\sigma}}_2^-$ and $\hat{\bar{\sigma}}_3^-$ could not degrade into nominal stress.

In order to overcome this limitation, a different pattern of stiffness degradation should be defined. To take the effective principal or normal stress in any principal direction as the resultant force of the axial stresses in three orthogonal directions, i.e.

$$\begin{Bmatrix} \hat{\sigma}_1 \\ \hat{\sigma}_2 \\ \hat{\sigma}_3 \end{Bmatrix} = \varpi \cdot \begin{Bmatrix} (1-\bar{\nu})\hat{\bar{\sigma}}_1' + \bar{\nu}\hat{\bar{\sigma}}_2' + \bar{\nu}\hat{\bar{\sigma}}_3' \\ \bar{\nu}\hat{\bar{\sigma}}_1' + (1-\bar{\nu})\hat{\bar{\sigma}}_2' + \bar{\nu}\hat{\bar{\sigma}}_3' \\ \bar{\nu}\hat{\bar{\sigma}}_1' + \bar{\nu}\hat{\bar{\sigma}}_2' + (1-\bar{\nu})\hat{\bar{\sigma}}_3' \end{Bmatrix} \tag{64}$$

with $\varpi(1-\bar{\nu})$ and $\varpi\bar{\nu}$ being contributing coefficient, and assuming that when damage occurs and the axial effective stresses degrade into nominal stresses, with the nominal principal or normal stress in any principal direction being the resultant force of the axial nominal stresses, i.e.

$$\begin{Bmatrix} \hat{\sigma}_1 \\ \hat{\sigma}_2 \\ \hat{\sigma}_3 \end{Bmatrix} = \varpi \cdot \begin{Bmatrix} (1-\bar{\nu})\hat{\sigma}_1^{'} + \bar{\nu}\hat{\sigma}_2^{'} + \bar{\nu}\hat{\sigma}_3^{'} \\ \bar{\nu}\hat{\sigma}_1^{'} + (1-\bar{\nu})\hat{\sigma}_2^{'} + \bar{\nu}\hat{\sigma}_3^{'} \\ \bar{\nu}\hat{\sigma}_1^{'} + \bar{\nu}\hat{\sigma}_2^{'} + (1-\bar{\nu})\hat{\sigma}_3^{'} \end{Bmatrix} \tag{65}$$

with $\hat{\sigma}_i^{'} = \phi_i \hat{\bar{\sigma}}_i^{'} (i = 1, 2, 3)$,then the matrix representation of damaged elastic stiffness tensor can be defined as:

where $\left[M^{\pm}(\hat{\omega}^{\pm})\right]$ can be expressed as:

$$\left[M^{\pm}\right] = dig\left[\phi_1^{\pm}\ \phi_2^{\pm}\ \phi_3^{\pm}\ \sqrt{\phi_2^{\pm}\phi_3^{\pm}}\ \sqrt{\phi_1^{\pm}\phi_3^{\pm}}\ \sqrt{\phi_1^{\pm}\phi_2^{\pm}}\right] \tag{73}$$

where $\phi_i^{\pm} = (1-\hat{\omega}_i^{\pm})^2$ with $\hat{\omega}_i^{\pm}(i = 1, 2, 3)$ being the principal tensile and compressive damage variables.

$$[E] = \varpi \cdot \begin{bmatrix} E_1(1-\bar{\nu}) & E_2\bar{\nu} & E_3\bar{\nu} & 0 & 0 & 0 \\ E_1\bar{\nu} & E_2(1-\bar{\nu}) & E_3\bar{\nu} & 0 & 0 & 0 \\ E_1\bar{\nu} & E_2\bar{\nu} & E_3(1-\bar{\nu}) & 0 & 0 & 0 \\ 0 & 0 & 0 & \frac{E_{23}(1-2\bar{\nu})}{2} & 0 & 0 \\ 0 & 0 & 0 & 0 & \frac{E_{13}(1-2\bar{\nu})}{2} & 0 \\ 0 & 0 & 0 & 0 & 0 & \frac{E_{12}(1-2\bar{\nu})}{2} \end{bmatrix}. \tag{66}$$

By this method, Eq. (47) can be rewritten as:

$$\begin{Bmatrix} \hat{\sigma}_1 \\ \hat{\sigma}_2 \\ \hat{\sigma}_3 \end{Bmatrix} = \varpi\left(\Upsilon^{'} + \Psi^{'}\right). \tag{67}$$

where $\Upsilon^{'}$ can be expressed as:

$$\Upsilon^{'} = \begin{bmatrix} (1-\bar{\nu}) & \phi_2^{+}\bar{\nu} & \phi_3^{+}\bar{\nu} \\ \bar{\nu} & \phi_2^{+}(1-\bar{\nu}) & \phi_3^{+}\bar{\nu} \\ \bar{\nu} & \phi_2^{+}\bar{\nu} & \phi_3^{+}(1-\bar{\nu}) \end{bmatrix} \begin{Bmatrix} 0 \\ \hat{\bar{\sigma}}_2^{'+} \\ \hat{\bar{\sigma}}_3^{'+} \end{Bmatrix}. \tag{68}$$

and $\Psi^{'}$ can be expressed as:

$$\Psi^{'} = \begin{bmatrix} \phi_1^{-}(1-\bar{\nu}) & \bar{\nu} & \bar{\nu} \\ \phi_1^{-}\bar{\nu} & (1-\bar{\nu}) & \bar{\nu} \\ \phi_1^{-}\bar{\nu} & \bar{\nu} & (1-\bar{\nu}) \end{bmatrix} \begin{Bmatrix} \hat{\bar{\sigma}}_1^{'-} \\ 0 \\ 0 \end{Bmatrix}. \tag{69}$$

By rearranging the above three equations, the following equation can be obtained:

$$\begin{Bmatrix} \hat{\sigma}_1 \\ \hat{\sigma}_2 \\ \hat{\sigma}_3 \end{Bmatrix} = \varpi \cdot \begin{Bmatrix} \phi_2^{+}\bar{\nu}\hat{\bar{\sigma}}_2^{'+} + \phi_3^{+}\bar{\nu}\hat{\bar{\sigma}}_3^{'+} + \phi_1^{-}(1-\bar{\nu})\hat{\bar{\sigma}}_1^{'-} \\ \phi_2^{+}(1-\bar{\nu})\hat{\bar{\sigma}}_2^{'+} + \phi_3^{+}\bar{\nu}\hat{\bar{\sigma}}_3^{'+} + \phi_1^{-}\bar{\nu}\hat{\bar{\sigma}}_1^{'-} \\ \phi_2^{+}\bar{\nu}\hat{\bar{\sigma}}_2^{'+} + \phi_3^{+}(1-\bar{\nu})\hat{\bar{\sigma}}_3^{'+} + \phi_1^{-}\bar{\nu}\hat{\bar{\sigma}}_1^{'-} \end{Bmatrix}. \tag{70}$$

From Eq. (70), it can be noted that the issue existing in Eq. (63) was avoided.

Through further analysis, it is seen that Eq. (66) can be decomposed as:

$$[E] = \left[\bar{E}\right][M] \tag{71}$$

where $\left[\bar{E}\right]$ is the initial undamaged elastic stiffness matrix and $[M]$ can be expressed by Eq. (42).

Then Eq. (59) can be rewritten as:

$$\{\sigma\} = \left[\bar{E}\right]\left[M^{+}\right]\left\{\varepsilon^{+e}\right\} + \left[\bar{E}\right]\left[M^{-}\right]\left\{\varepsilon^{-e}\right\} \tag{72}$$

The damage–effect matrix shown in Eq. (73) is in the principal coordinate system of damage which corresponds to the direction of the principal strains. In terms of a general coordinate system, it should be transformed to the global coordinate system as following:

$$\left[M_*^{\pm}(\hat{\omega})\right] = [R]^T\left[M^{\pm}\right][R] \tag{74}$$

where $[R]$ is the coordinate transition matrix.

By substituting Eq. (74) into Eq. (72), Eq. (72) can be rewritten as:

$$\{\sigma\} = \left[\bar{E}\right]\left[M_*^{+}\right]\left\{\varepsilon^{+e}\right\} + \left[\bar{E}\right]\left[M_*^{-}\right]\left\{\varepsilon^{-e}\right\}. \tag{75}$$

2. Definition of damaged elastic stiffness for cyclic loading

Tests of concrete showed that the degradation of the elastic stiffness had unilateral effect under cyclic loading due to the opening and closing of micro cracks caused by the load that changed the sign during the loading process. It can be explained that some tensile cracks tended to close when the load changed from tension to compression, which led to elastic stiffness recovery during compressive loading; whereas, in the case of transition from compression to tension, the pre-existing cracks formed during the previous compressive loading and the new cracks formed during the subsequent tensile loading would cause further reduction of the elastic stiffness. Because the damage-effect matrix $\left[M_*^{\pm}\right]$ defined in Eq. (75) did not include the elastic stiffness recovery phenomenon, the formulation proposed by Lee and Fenves (1998) for cyclic loading was extended in this paper for the anisotropic damage.

When the load changes from compression to tension, the anisotropic tensile damage variable will be assumed as follows:

$$\hat{w}_i^{+} = 1 - (1 - H(\hat{\varepsilon}_i)\hat{\omega}_i^{+})(1 - H(\hat{\varepsilon}_i)\hat{\omega}_i^{-}) \tag{76}$$

where $\hat{w}_i^+$ is the tensile damage variable for cyclic loading and $H(x)$ is the Heaviside step function ($H(x) = 1$ for $x > 0$ and $H(x) = 0$ for $x < 0$).

For the case of transition from tension to compression, the anisotropic compressive damage variable is defined as:

$$\hat{w}_i^- = 1 - (1 - H(-\hat{\varepsilon}_i)s_0\hat{\omega}_i^-)(1 - H(-\hat{\varepsilon}_i)\hat{\omega}_i^-) \quad (77)$$

where $\hat{w}_i^-$ is the compressive damage variable for cyclic loading and $0 \le s_0 \le 1$ is a constant. Any value between 0 and 1 will result in partial recovery of the elastic stiffness.

Based on Eqs. (76) and (77), the following can be obtained:

a. when all principal strains are positive, $H(\hat{\varepsilon}_i) = 1$ and Eq. (76) becomes

$$\hat{w}_i^+ = 1 - (1 - \hat{\omega}_i^+)(1 - \hat{\omega}_i^-) = \hat{\omega}_i^+ + \hat{\omega}_i^- - \hat{\omega}_i^+\hat{\omega}_i^- \quad (78)$$

which implies that there is no stiffness recovery occurs when the load changes from compression to tension.

b. when all principal strains are negative, $H(\hat{\varepsilon}_i) = 0$ and $H(-\hat{\varepsilon}_i) = 1$ and Eq. (76) can be simplified down to $\hat{w}_i^+ = 0$, then Eq. (77) becomes

$$\hat{w}_i^- = 1 - (1 - s_0\hat{\omega}_i^+)(1 - \hat{\omega}_i^-) \quad (79)$$

which can reduce to $\hat{w}_i^- = \hat{\omega}_i^-$ when $s_0 = 0$, and it implies full elastic stiffness recovery during the transition from tension to compression. If $s_0 = 1$, Eq. (79) will reduce to the form of Eq. (78), which means that there is no stiffness recovery. For the case of $0 < s_0 < 1$, Eq. (79) can be written as $\hat{w}_i^- = s_0\hat{\omega}_i^+ + \hat{\omega}_i^- - s_0\hat{\omega}_i^+\hat{\omega}_i^-$, and it can be explained that some tensile cracks tend to close or partially close and as a result, elastic stiffness partial recovery occurs in compressive loading. To simplify the calculation, in this paper, the value of s_0 was set to one, i.e. full elastic stiffness recovery during the transition from tension to compression.

As mentioned above, if $\hat{\varepsilon}_1 > 0$, $\hat{\varepsilon}_2 < 0$ and $\hat{\varepsilon}_3 < 0$, then the following can be obtained:

$$\begin{aligned} &\hat{w}_1^+ = \hat{\omega}_1^+ + \hat{\omega}_1^- - \hat{\omega}_1^+\hat{\omega}_1^-, \quad \hat{w}_1^- = 0 \\ &\hat{w}_2^+ = 0, \quad \hat{w}_2^- = s_0\hat{\omega}_2^+ + \hat{\omega}_2^- - s_0\hat{\omega}_2^+\hat{\omega}_2^-. \\ &\hat{w}_3^+ = 0, \quad \hat{w}_3^- = s_0\hat{\omega}_3^+ + \hat{\omega}_3^- - s_0\hat{\omega}_3^+\hat{\omega}_3^- \end{aligned} \quad (80)$$

By substituting $\hat{w}_i^+$ and $\hat{w}_i^-$ into $\left[M^{\pm}\right]$ defined in Eq. (73), the damage-effect matrix for cyclic loading can be rewritten as follows:

$$\left[M_C^{\pm}(\hat{w}_i^{\pm})\right] = dig\left[\, \vartheta_1^{\pm}\ \vartheta_2^{\pm}\ \vartheta_3^{\pm}\ \sqrt{\vartheta_2^{\pm}\vartheta_3^{\pm}}\ \sqrt{\vartheta_1^{\pm}\vartheta_3^{+}}\ \sqrt{\vartheta_1^{\pm}\vartheta_2^{\pm}}\,\right] \quad (81)$$

where $\vartheta_i^+ = (1 - H(\hat{\varepsilon}_i)\hat{\omega}_i^+)(1 - H(\hat{\varepsilon}_i)\hat{\omega}_i^-)$ and $\vartheta_i^- = (1 - H(-\hat{\varepsilon}_i)s_0\hat{\omega}_i^+)(1 - H(-\hat{\varepsilon}_i)\hat{\omega}_i^-)$ with $\hat{\omega}_i^+$ and $\hat{\omega}_i^-$ being respectively the principal tensile and compressive damage variables and $i = 1, 2, 3$.

Combining Eqs. (71), (74) and (81), the final form of the damaged elastic stiffness for cyclic loading can be expressed as:

$$\left[E_C^{\pm}\right] = \left[\bar{E}\right][R]^T\left[M_C^{\pm}\right][R]. \quad (82)$$

2.2 Plasticity Part

Concrete has different material behaviors under tensile and compressive loadings, thus the yield criterion proposed by Lubliner et al. (1989) that accounts for both tension and compression plasticity was adopted in this work. This criterion was successful in simulating the concrete behavior under uniaxial, biaxial, multiaxial and cyclic loadings (Lee and Fenves 1998; Yu et al. 2010; Cicekli et al. 2007; Abu Al-Rub and Kim 2010; Shen et al. 2015). Furthermore, it was proved by Abu Al-Rub and Voyiadjis (2003) that PDMs formulated in the effective space were numerically more stable and attractive. In many works, this strategy was adopted (Abu Al-Rub and Kim 2010; Grassl et al. 2013; Liu et al. 2013; Murakami 2012), so was in this paper. Thus the yield criterion proposed by Lubliner et al. (1989) is expressed in the effective configuration as follows:

$$\begin{aligned} f = &\sqrt{3\bar{J}_2} + \alpha\bar{I}_1 + \beta(k_i^p)H(\hat{\bar{\sigma}}_{\max}) \\ &- (1-\alpha)\bar{c}^-(\varepsilon_{eq}^-) \le 0 \end{aligned} \quad (83)$$

where $\bar{J}_2 = \bar{s}_{ij}\bar{s}_{ij}/2$ is the second-invariant of the effective deviatoric stress tensor $\bar{s}_{ij} = \bar{\sigma}_{ij} - \bar{\sigma}_{kk}\delta_{ij}/3$, $\bar{I}_1 = \bar{\sigma}_{kk}$ is the first-invariant of the effective Cauchy stress tensor $\bar{\sigma}_{ij}$, $\hat{\bar{\sigma}}_{\max}$ is the maximum principal effective stress, $H(\hat{\bar{\sigma}}_{\max})$ is the Heaviside step function, and the parameters α and β are dimensionless constants which are defined by Lubliner et al. (1989) as follows:

$$\alpha = \frac{(f_{b0}/f_0^-) - 1}{2(f_{b0}/f_0^-) - 1}, \quad \beta = (1-\alpha)\frac{\bar{c}^-(\varepsilon_{eq}^-)}{\bar{c}^+(\varepsilon_{eq}^+)} - (1+\alpha) \quad (84)$$

with f_{b0} and f_0^- being respectively the initial equi-biaxial and uniaxial compressive yield stress. Experimental values for f_{b0}/f_0^- lie between 1.10 and 1.16 and yielding values for α are between 0.08 and 0.12. Referring to Abu Al-Rub and Kim (2010) 0.12 was chosen as the value for α in this study.

The internal plastic state variable k_i^p in Eq. (83) can be defined as follows:

$$k_i^p = \int_0^t \dot{k}_i^p dt = \int_0^t \dot{\lambda}^p B^P\left(\hat{\bar{\boldsymbol{\sigma}}}\right) dt \tag{85}$$

with its rate being expressed as

$$\dot{k}_i^p = H_{ij}\hat{\dot{\varepsilon}}_j^p \tag{86}$$

or

$$\begin{Bmatrix} \dot{\varepsilon}_{eq}^+ \\ 0 \\ \dot{\varepsilon}_{eq}^- \end{Bmatrix} = \begin{bmatrix} H^+ & 0 & 0 \\ 0 & 0 & 0 \\ 0 & 0 & H^- \end{bmatrix} \begin{Bmatrix} \hat{\dot{\varepsilon}}_1^P \\ \hat{\dot{\varepsilon}}_2^P \\ \hat{\dot{\varepsilon}}_3^P \end{Bmatrix} \tag{87}$$

where H^+ and H^- are defined as

$$H^+ = r(\hat{\bar{\sigma}}_{ij}) \tag{88}$$

and

$$H^- = -(1 - r(\hat{\bar{\sigma}}_{ij})) \tag{89}$$

The dimensionless parameter $r(\hat{\bar{\sigma}}_{ij})$ is a weight factor which can be expressed as follows:

$$r(\hat{\bar{\sigma}}_{ij}) = \frac{\sum_{k=1}^3 \left\langle \hat{\bar{\sigma}}_k \right\rangle}{\sum_{k=1}^3 \left| \hat{\bar{\sigma}}_k \right|} \tag{90}$$

where the sign $\langle \bullet \rangle$ indicates Macauley bracket, which is defined as

$$\langle x \rangle = \frac{1}{2}(|x| + x), k = 1, 2, 3. \tag{91}$$

In fact, $\dot{\varepsilon}_{eq}^+$ and $\dot{\varepsilon}_{eq}^-$ are equivalent to the following two equations:

$$\dot{\varepsilon}_{eq}^+ = r(\hat{\bar{\sigma}}_{ij})\hat{\dot{\varepsilon}}_{\max}^p \tag{92}$$

and

$$\dot{\varepsilon}_{eq}^- = -(1 - r(\hat{\bar{\sigma}}_{ij}))\hat{\dot{\varepsilon}}_{\min}^p \tag{93}$$

where $\hat{\dot{\varepsilon}}_{\max}^p$ and $\hat{\dot{\varepsilon}}_{\min}^p$ are respectively the maximum and minimum eigenvalues of the plastic strain rate $\dot{\varepsilon}_{ij}^p$. If $\hat{\dot{\varepsilon}}_1^p > \hat{\dot{\varepsilon}}_2^p > \hat{\dot{\varepsilon}}_3^p$, then $\hat{\dot{\varepsilon}}_{\max}^p = \hat{\dot{\varepsilon}}_1^p$ and $\hat{\dot{\varepsilon}}_{\min}^p = \hat{\dot{\varepsilon}}_3^p$ and $\hat{\dot{\boldsymbol{\varepsilon}}}^p$ can be expressed as:

$$\hat{\dot{\boldsymbol{\varepsilon}}}^p = \left[\, \hat{\dot{\varepsilon}}_1^p \;\; \hat{\dot{\varepsilon}}_2^p \;\; \hat{\dot{\varepsilon}}_3^p \,\right]^T = \dot{\lambda}^p \frac{\partial G^p\left(\hat{\bar{\boldsymbol{\sigma}}}\right)}{\partial \hat{\bar{\boldsymbol{\sigma}}}} \tag{94}$$

where G^P is the plastic potential, which is to be described later.

Combining Eqs. (87) and (94), the expression $B^p(\hat{\bar{\boldsymbol{\sigma}}})$ in Eq. (85) can be obtained as

$$B^p\left(\hat{\bar{\boldsymbol{\sigma}}}\right) = \begin{bmatrix} r\left(\hat{\bar{\boldsymbol{\sigma}}}\right) & 0 & 0 \\ 0 & 0 & 0 \\ 0 & 0 & -\left(1 - r\left(\hat{\bar{\boldsymbol{\sigma}}}\right)\right) \end{bmatrix} \cdot \frac{\partial G^p\left(\hat{\bar{\boldsymbol{\sigma}}}\right)}{\partial \hat{\bar{\boldsymbol{\sigma}}}}. \tag{95}$$

Since concrete behavior in compression is more of a ductile behavior as compared to its corresponding brittle behavior in tension (Abu Al-Rub and Kim 2010), the isotropic hardening expressions $\bar{c}^+$ and $\bar{c}^-$ in the effective configuration are defined as follows:

$$\bar{c}^+ = \bar{f}_0^+ + h^+ \varepsilon_{eq}^+ \tag{96}$$

$$\bar{c}^- = -\bar{f}_0^- + Q^- \left[1 - \exp(-b^- \varepsilon_{eq}^-)\right] \tag{97}$$

where $\bar{f}_0^+$ and $\bar{f}_0^-$ ($\bar{f}_0^- < 0$) are respectively the effective yield strengths under uniaxial tension and compression. The parameters Q^-, b^- and h^+ are material constants, which are obtained in the effective configuration of the uniaxial cycle stress–strain diagram.

In view of the material property of concrete, in the present model, the flow rule is given as a function of the effective stress $\bar{\sigma}_{ij}$, such that:

$$\dot{\varepsilon}_{ij}^p = \dot{\lambda}^p \frac{\partial G^p}{\partial \bar{\sigma}_{ij}} \tag{98}$$

where $\dot{\lambda}^p$ is the Lagrangian plasticity multiplier, which can be obtained under the plasticity consistency condition, $\dot{f} = 0$, such that

$$f \le 0, \dot{\lambda}^p \ge 0, \dot{\lambda}^p f = 0, \dot{\lambda}^p \dot{f} = 0. \tag{99}$$

The plastic potential G^p adopted in this paper is the Drucker-Prager function expressed as:

$$G^p = \sqrt{3\bar{J}_2} + \alpha^p \bar{I}_1 \tag{100}$$

where α^p is a parameter chosen to provide proper distance with common range between 0.2 and 0.3 for concrete, and the plastic flow direction $\partial G^p/\partial \bar{\sigma}_{ij}$ in Eq. (100) can be expressed as

$$\frac{\partial G^p}{\partial \bar{\sigma}_{ij}} = \frac{3}{2} \frac{\bar{s}_{ij}}{\sqrt{3\bar{J}_2}} + \alpha^p \delta_{ij}. \tag{101}$$

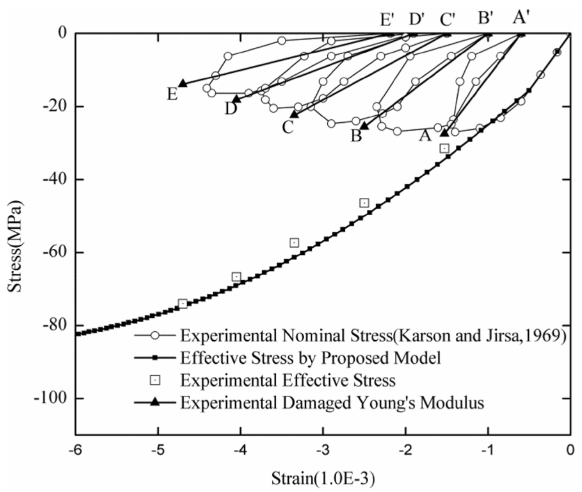

Fig. 5 Experimental stress–strain curves in the effective and nominal configurations for Karsan and Jirsa (1969) experimental data.

3 Calibration and Comparisons with Test Results

To investigate the applicability and effectiveness of the proposed model, several numerical examples of concrete under different loading conditions were presented in this section. The model response was compared with five groups of experiments including cyclic, uniaxial, and biaxial loading.

The calibration of the material parameters often relies on monotonic stress–strain experimental curves. However, this method results in a non-unique determination of these material parameters. Therefore, based on the uniaxial cyclic test, Abu Al-Rub and Kim (2010) proposed a method to identify the plasticity material parameters. The method can be summarized as follows: Firstly, the damaged Young's module E for each cycle can be determined by connecting each unloading points $(A-E)$ and reloading points $(A^{'}-E^{'})$ shown in Fig. 5. Then the effective stress $\bar{\sigma}$ can be obtained by the equation as $\bar{\sigma}=(\bar{E}/E)\sigma$. Under this condition, the plasticity parameters h^{+}, Q^{-} and b^{-} can be determined. Moreover, from Eq. (8) and the measured damaged Young's module in Fig. 5, the variation of the damage density with strain can be plotted shown in Fig. 6b such that $d=1-E/\bar{E}_{0}$. For more details of this method, Abu Al-Rub and Kim (2010) can be referred. As mentioned previously, since the uniaxial cyclic tests are relatively complex, the stress–strain data is usually obtained by uniaxial monotonic test in actual engineering. Therefore, the method proposed by Abu Al-Rub and Kim (2010) to identify the plasticity parameters may cause the lack of uniaxial cyclic loading stress–strain data. Based on the above analysis, the following method was used to identify the plasticity parameters in this study, and it can be summarized as follows: Firstly, based on Eqs. (16) and (20), the relations between stress and strain under uniaxial stress state can be obtained. With Eqs. (19) and (23), the damage variables d^{+} and d^{-} can be determined. However, since the axial plastic strains $\varepsilon^{\pm p}$ are unknowns in the computing processes of the damage variables d^{+} and d^{-}, in order to obtain the damage variables, the axial plastic strains should be determined firstly. As discussed in Zhang et al. (2008), the ratio of axial plastic strain ε^{+p} and inelastic strain ε^{+ck} under uniaxial tension can be taken as 0.50–0.95 and the ratio of axial plastic strain ε^{-p} and inelastic strain ε^{-in} under uniaxial compression can be taken as 0.35–0.70. As shown in Fig. 1, the inelastic strains ε^{+ck} and ε^{-in} can be obtained by the following equations:

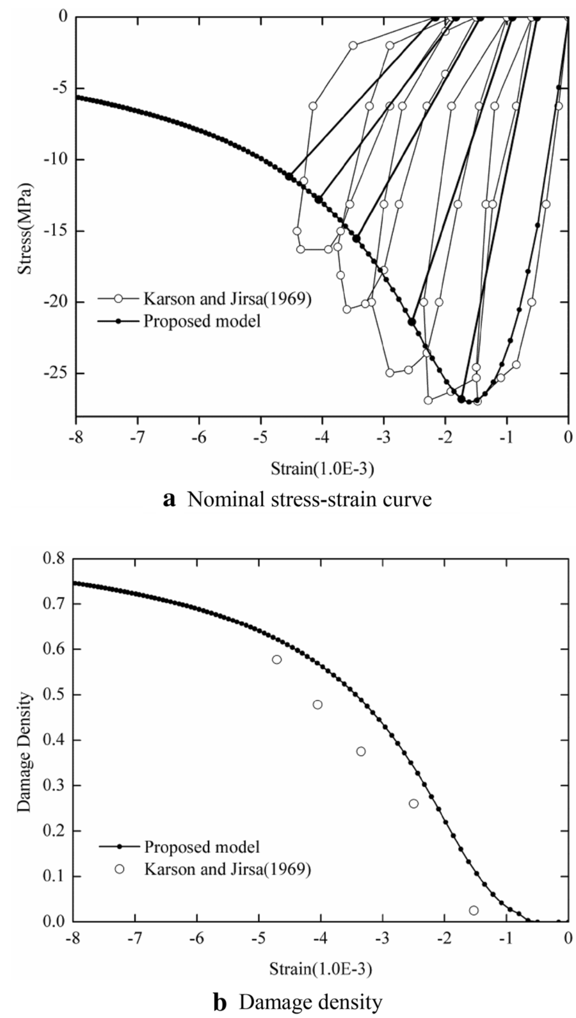

Fig. 6 The model responses in cyclic compression compared to experimental results presented in Karsan and Jirsa (1969).

$$\varepsilon^{+ck}=\varepsilon^{+}-\sigma^{+}/\bar{E}_{0},\quad \varepsilon^{-in}=\varepsilon^{-}-\sigma^{-}/\bar{E}_{0}. \tag{102}$$

Table 1 Material constants identified from the experimental results (Karsan and Jirsa 1969).

E_0(Gpa)	ν	f_u^- (MPa)	ε_u^- (1.0E−3)
31.00	0.20	− 27.00	−1.59
α_a	α_d	Q^-(MPa)	b^-
2.06	1.18	74.00	702.14

Table 2 Material constants identified from the experiment results of Taylor (1992).

E_0(Gpa)	ν	f_0^+(MPa)
31.00	0.2	3.40
ε_0^+(1.0E−4)	α_t	h^+(MPa)
1.26	3.61	4436

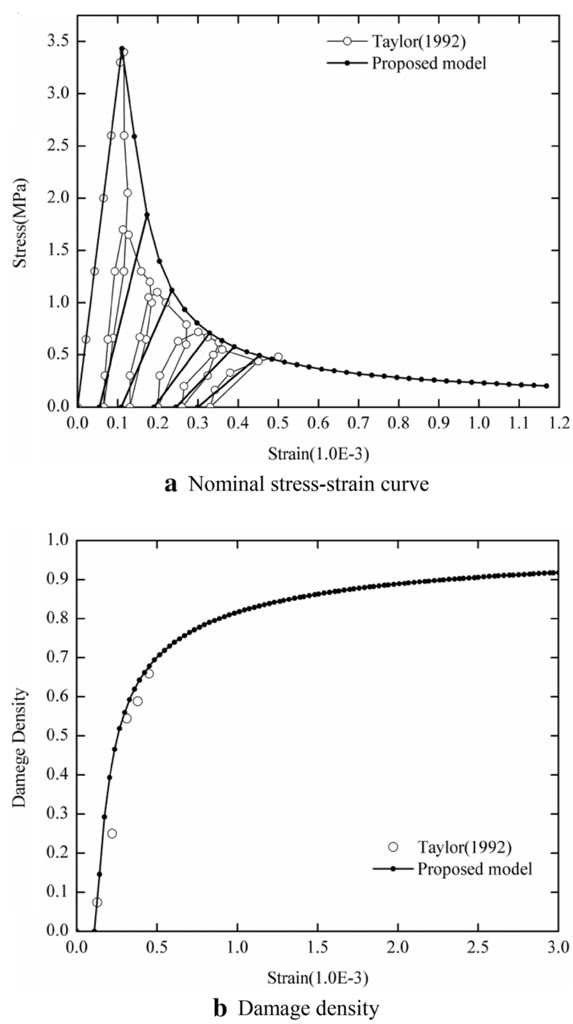

Fig. 7 The model responses in cyclic tension compared to experimental results presented in Taylor (1992).

In this study, based on the experimental results of uniaxial cyclic tensile test of Taylor (1992) and uniaxial cyclic compressive test of Karsan and Jirsa (1969), the ratio of axial plastic strain ε^{+p} and inelastic strain ε^{+ck} was taken as 0.90, and the ratio of axial plastic strain $\varepsilon^{-p}$and inelastic strain ε^{-in} was taken as 0.60. With this, the damage variables d'^{+} and d'^{-} by using Eqs. (19) and (23) can be obtained, and then the effective stress $\bar{\sigma}$ can be obtained by using Eq. (1). Based on the above analysis, the plasticity material parameters can be obtained by fitting the calculated effective stress-axial plastic strain curve.

3.1 Uniaxial Cyclic Compressive Test

Using the method mentioned above, the identified compressive plasticity and damage material constants associated with fitting Karsan and Jirsa (1969) experimental data are listed in Table 1. The comparison between the numerical predictions and the experiment results is shown in Figs. 5 and 6.

From Fig. 5, it can be seen that the predicted effective stress–strain curve is in line with the experiment result. However, Fig. 6a shows that the predicted nominal stress

Table 3 Material properties used for the monotonic uniaxial compressive test.

E_0(Gpa)	ν	f_u^-(MPa)	ε_u^- (1.0E−3)
31.70	0.20	−27.63	−1.60
α_a	α_d	Q^-(MPa)	b^-
2.05	1.22	37.00	3173

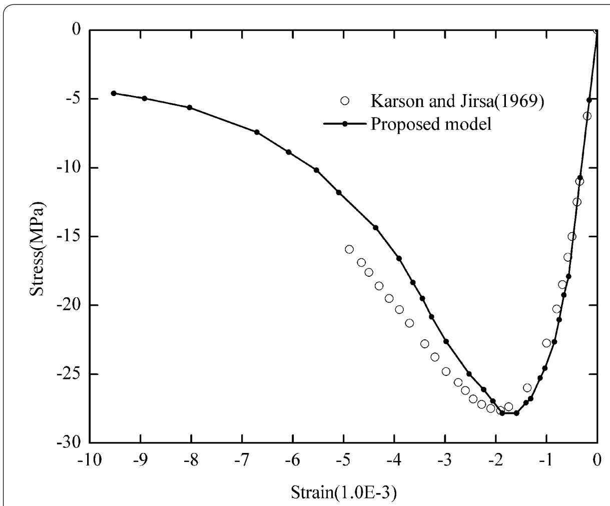

Fig. 8 The model responses in monotonic uniaxial compression compared to experimental results presented in Karsan and Jirsa (1969).

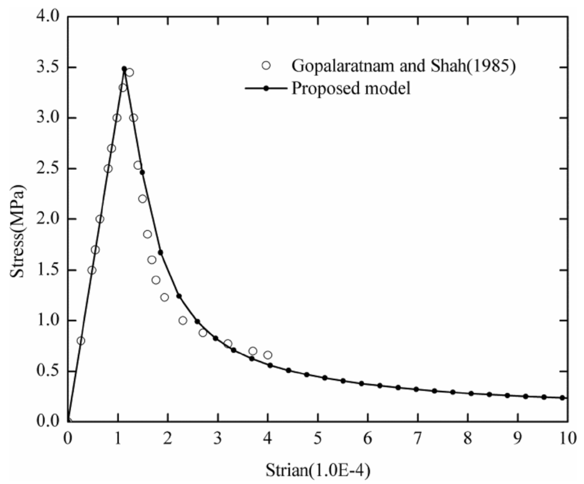

Fig. 9 The model responses in monotonic uniaxial tension compared to experimental results presented in Gopalaratnam and Shah (1985).

is slightly smaller than the experiment result. The main reason is that the predicted damage density is higher than the value showed in the experiment result under the same strain (see Fig. 6b). Although the damage density is slightly higher than the predicted value, the calculated result is reasonable because the bigger predicted damage value is safer in project.

3.2 Uniaxial Cyclic Tensile Test

With the same method mentioned above, the identified material parameters are listed in Table 2. The experiment results of uniaxial cyclic tensile test of Taylor (1992) are compared with the numerical predictions shown in Fig. 7. From Fig. 7, it can be seen that the predicted nominal stress–strain curve and the damage density agree with the experiment results.

3.3 Monotonic Uniaxial Compressive Test

The experiment results of uniaxial compressive test (Karsan and Jirsa 1969) were employed in this paper for comparison. The material properties adopted in the simulation are listed in Table 3. The comparison between the simulation and test is presented in Fig. 8. From Fig. 8, it can be seen that the predicted nominal stress is slightly smaller than the value showed in the experiment result. This phenomenon is also caused by the bigger predicted damage density.

Table 4 Material parameters used for the monotonic uniaxial tensile test.

E_0(Gpa)	ν	f_0^+(MPa)
31.00	0.2	3.45
ε_0^+(1.0E−4)	α_t	h^+(MPa)
1.27	3.71	10,304

3.4 Monotonic Uniaxial Tensile Test

The comparison between the numerical predictions and the experimental results of Gopalaratnam and Shah (1985) is presented in Fig. 9. The material constants used in this simulation are listed in Table 4. As it is shown in Fig. 9, the simulated tensile stress–strain curve agrees with the experimental data.

3.5 Monotonic Biaxial Compressive Test

The biaxial compressive test presented in Kupfer et al. (1969) was adopted in this paper to validate the model. The comparison between the numerical predictions and the experimental results is presented in Fig. 10. The material constants for numerical simulation are listed in Table 5.

In this paper, the strain tensor was decomposed into positive and negative parts by spectrum decomposition technique and the corresponding stress tensor was split into two parts. Through this processing, not only the different damage responses can be considered, but also the Poisson's effect can be easily considered in the biaxial or trial compression test. As it is shown in Fig. 10c, when the biaxial stress ratio is $\sigma_1/\sigma_2 = -1/-0.52$, both$\varepsilon_1$ and$\varepsilon_2$will be compressive strains and $\varepsilon_3$will be the tensile strain. Since tensile strain may lead to tensile damage, to consider tensile material constants is indispensable in this case. This is both an advantage and a disadvantage. The advantage is that the model can accurately characterize damage anisotropic of concrete under multi-axial stress state with the Poisson's effect taken into account, and the disadvantage is that more material constants are needed.

4 Conclusions

Based on the combination of damage mechanics and classical plastic theory, a new empirical plastic–damage constitutive model was presented to simulate the failure of concrete. The proposed model could include different responses of concrete under tension and compression, the effect of stiffness degradation, the interaction effects of damage in the orthogonal direction and the stiffness

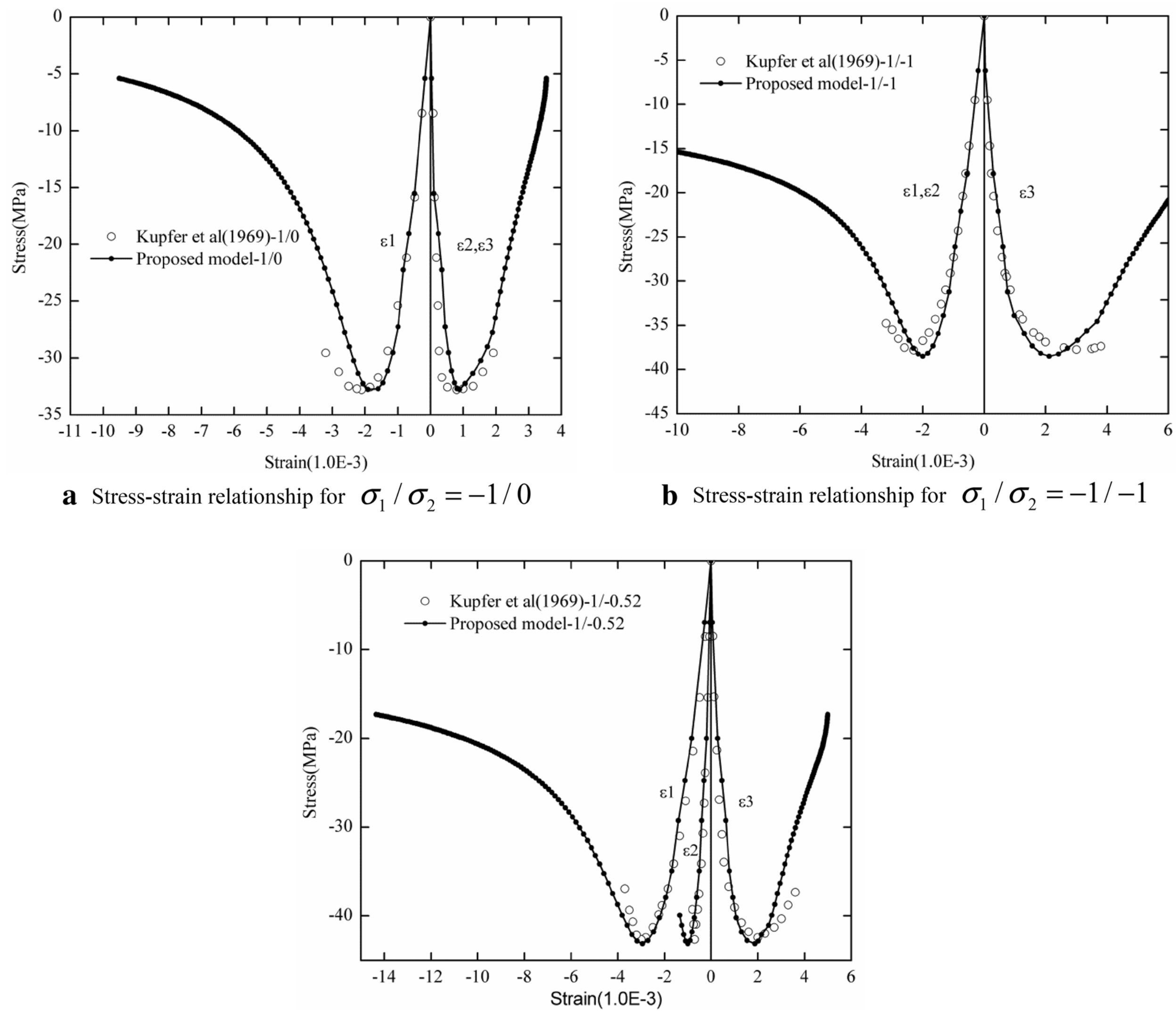

a Stress-strain relationship for $\sigma_1/\sigma_2=-1/0$

b Stress-strain relationship for $\sigma_1/\sigma_2=-1/-1$

c Stress-strain relationship for $\sigma_1/\sigma_2=-1/-0.52$

Fig. 10 The model responses in monotonic uniaxial and biaxial compressive loading compared to experimental results reported by Kupfer et al. (1969).

Table 5 Material constants used for the biaxial compressive test.

Elastic constants		**Tensile material constants**			
E_0(Gpa)	ν	f_0^+(MPa)	ε_0^+(1.0E−4)	α_t	h^+(MPa)
32.00	0.20	2.88	1.15	2.59	8112
Compressive material constants					
f_u^-(MPa)	ε_u^-(1.0E−3)	α_a	α_d	Q^-(MPa)	b^-
−32.80	−1.69	1.99	1.53	70.24	892.51

recovery due to crack closure in cyclic loading. With comparison with a wide range of experiment results, it was concluded that:

1. The proposed model could effectively simulate the nonlinear properties of concrete under different loading conditions, such as cyclic, uniaxial and biaxial conditions. Moreover, the proposed model could overcome the limitation of lack of uniaxial cyclic loading stress–strain data in actual engineering and could determine the parameters conveniently.
2. Although choosing strain as the state variable to judge the damage state is a controversial issue, the

results of simulation in this paper indicated that this choice was feasible. Moreover, although more material constants are needed with the Poisson's effect in the multi-axial compressive test being considered, to give an eye to tensile material constants was indispensable.

Acknowledgements
The authors are grateful to the support of National Natural Science Foundation of China (No. 51709116), the Priority Academic Program Development of Jiangsu Higher Education Institutions (No. 3014-SYS1401), the Key Scientific Research Projects of Henan Province Universities and Colleges (No. 17B570003) and Foundation for Dr in North China University of Water Resources and Electric Power (No. 10030 and 40589). Special thanks for the reviewers and their constructive comments and suggestions in improving the quality of this manuscript.

Authors' contributions
Z-ZS conceived and designed the study. Y-TJ wrote the paper. BW reviewed and edited the manuscript. All authors read and approved the final manuscript.

Competing interests
The authors declare that they have no competing interests.

Author details
[1] School of Water Conservancy, North China University of Water Resources and Electric Power, Zhengzhou 450045, China. [2] Hohai University, Nanjing 210098, China.

Received: 7 November 2017 Accepted: 6 June 2019
Published online: 30 September 2019

References

Abu Al-Rub, R. K., & Kim, S. M. (2010). Computational applications of a coupled plasticity–damage constitutive model for simulating plain concrete fracture. *Engineering Fracture Mechanics, 77,* 1577–1603.

Abu Al-Rub, R. K., & Voyiadjis, G. Z. (2003). On the coupling of anisotropic damage and plasticity models for ductile materials. *International Journal of Solids and Structures, 40,* 2611–2643.

Al-Rub, A., Rashid, K., Darabi, M. K., Kim, S.-M., Dallas, N., Glover, et al. (2013). Mechanistic-based constitutive modeling of oxidative aging in aging-susceptible materials and its effect on the damage potential of asphalt concrete. *Construction & Building Materials, 41,* 439–454.

Berto, L., Saetta, A., Scotta, R., & Talledo, D. (2014). A coupled damage model for RC structures: Proposal for a frost deterioration model and enhancement of mixed tension domain. *Construction & Building Materials, 65,* 310–320.

Carol, I., Rizzi, E., & Willam, K. (2001). On the formulation of anisotropic elastic degradation. I. Theory based on a pseudo-logarithmic damage tensor rate. *International Journal of Solids & Structures, 38,* 491–518.

Challamel, N., Lanos, C., & Casandjian, C. (2005). Strain-based anisotropic damage modelling and unilateral effects. *International Journal of Mechanical Sciences, 47,* 459–473.

Chow, C., & Wang, J. (1987). An anisotropic theory of elasticity for continuum damage mechanics. *International Journal of Fracture, 33,* 3–16.

Cicekli, U., Voyiadjis, G. Z., & Abu Al-Rub, R. K. (2007). A plasticity and anisotropic damage model for plain concrete. *International Journal of Plasticity, 23,* 1874–1900.

Cordebois, J. P., & Sidoroff, F. (1982). *Damage Induced Elastic Anisotropy*. Dordrecht: Springer, Netherlands.

Faria, R., Oliver, J., & Cervera, M. (1998). A strain-based plastic viscous–damage model for massive concrete structures. *International Journal of Solids and Structures, 35,* 1533–1558.

Gao, Z.-G., Huang, D.-H., & Zhao, G.-F. (2001). An orthotropic damage constitutive model for RCC. *Journal of Hydraulic Engineering, 244,* 58–64.

Gopalaratnam, V., & Shah, S. P. (1985). Softening response of plain concrete in direct tension. *ACI Journal, 82,* 310–323.

Grassl, P., & Jir Sek, M. (2006a). Damage-plastic model for concrete failure. *International Journal of Solids and Structures, 43,* 7166–7196.

Grassl, P., & Jir Sek, M. (2006b). Plastic model with non-local damage applied to concrete. *International Journal for Numerical and Analytical Methods in Geomechanics, 30,* 71–90.

Grassl, P., Xenos, D., Nystr, M., Rempling, R., & Gylltoft, K. (2013). CDPM2: A damage–plasticity approach to modelling the failure of concrete. *International Journal of Solids and Structures, 50,* 3805–3816.

Hesebeck, O. (2001). On an isotropic damage mechanics model for ductile materials. *International Journal of Damage Mechanics, 10,* 325–346.

Karsan, I. D., & Jirsa, J. O. (1969). Behavior of concrete under compressive loadings. *Journal of the Structural Division (ASCE), 95,* 2543–2563.

Kitzig, M., & Häußler-Combe, U. (2011). Modeling of plain concrete structures based on an anisotropic damage formulation. *Materials and Structures, 44,* 1837–1853.

Kupfer, H., Hilsdorf, H. K., & Rusch, H. (1969). Behavior of concrete under biaxial stresses. *Journal of the American Concrete Institute, 66,* 656–666.

Lee, J. H., & Fenves, G. L. (1998). Plastic–damage model for cyclic loading of concrete structures. *Journal of Engineering Mechanics-Asce, 124,* 892–900.

Lemaitre, J. L. & Chanboche, J. L. (1974). A nonlinear model of creep-fatigue damage cumulation and interaction. In *Proceeding of TUTAM Symposium of Mechanics of Visco-elasticity Media and Bodies, 1974*. Gotenbourg: Springer

Liu, J., Liu, R., & Zhong, H. (2013). An elastoplastic damage constitutive model for concrete. *China Ocean Engineering, 27,* 169–182.

Lubliner, J., Oliver, J., Oller, S., & Ate, E. (1989). A plastic–damage model for concrete. *International Journal of Solids and Structures, 25,* 299–326.

Mahnken, R. (2002). Theoretical, numerical and identification aspects of a new model class for ductile damage. *International Journal of Plasticity, 18,* 801–831.

Mazars, J., & Pijaudier-Cabot, G. (1989). Continuum damage theory—application to concrete. *Journal of Engineering Mechanics ASCE, 115,* 345–365.

Ministry of Construction. (2002). *Code for design of concrete structures (GB50010-2002)*. Beijing: China Building Industry Press.

Mozaffari, N., & Voyiadjis, G. Z. (2015). Phase field based nonlocal anisotropic damage mechanics model. *Physica D Nonlinear Phenomena, 308,* 11–25.

Murakami, S. (2012). *Continuum damage mechanics: A continuum mechanics approach to the analysis of damage and fracture*. Berlin: Springer.

Peng, J., Zhao, G., & Zhu, Y.-H. (1997). Studies of multiaxial shear strengths for roller-compacted concrete. *ACI Structural Journal, 94,* 114–123.

Prochtel, P., & Häußler-Combe, U. (2008). On the dissipative zone in anisotropic damage models for concrete. *International Journal of Solids and structures, 45,* 4384–4406.

Rabotnov, Y. N. (1968) Published. Creep rupture. In *Proceedings of the XII International Congress on Applied Mechanics, 1968 Stanford.* (pp. 342–349). Berlin: Springer

Shen, L., Ren, Q., Xia, N., Sun, L., & Xia, X. (2015). Mesoscopic numerical simulation of effective thermal conductivity of tensile cracked concrete. *Construction & Building Materials, 95,* 467–475.

Taqieddin, Z. N., Voyiadjis, G. Z., & Almasri, A. H. (2012). Formulation and verification of a concrete model with strong coupling between isotropic damage and elastoplasticity and comparison to a weak coupling model. *Journal of Engineering Mechanics, 138,* 530–541.

Taylor, R. (1992). *FEAP: A finite element analysis program for engineering workstation*. Berkeley: Department of Civil Engineering, University of California.

Valentini, B., & Hofstetter, G. (2013). Review and enhancement of 3D concrete models for large-scale numerical simulations of concrete structures. *International Journal for Numerical and Analytical Methods in Geomechanics, 37,* 221–246.

van Mier, J. G. M. (1984). *Strain-softening of concrete under multiaxial loading conditions* (Ph.D. Thesis). Eindhoven: Technische Hogeschool Eindhoven.

Voyiadjis, G. Z., & Deliktas, B. (2000). A coupled anisotropic damage model for the inelastic response of composite materials. *Computer Methods in Applied Mechanics and Engineering, 183,* 159–199.

Voyiadjis, G. Z., Taqieddin, Z. N., & Kattan, P. I. (2008). Anisotropic damage–plasticity model for concrete. *International Journal of Plasticity, 24,* 1946–1965.

Wu, J., Jie, L., & Faria, R. (2006). An energy release rate-based plastic–damage model for concrete. *International Journal of Solids and Structures, 43,* 583–612.

Yu, T., Teng, J. G., Wong, Y. L., & Dong, S. L. (2010). Finite element modeling of confined concrete-II: Plastic–damage model. *Engineering Structures, 32,* 680–691.
Zhang, W., Chen, Y., & Jin, Y. (2001). Effects of symmetrisation of net-stress tensor in anisotropic damage models. *International Journal of Fracture, 109,* 345–363.
Zhang, J., Wang, Q., Hu, S., & Wang, C. (2008). Parameters verification of concrete damaged plastic model of Abaqus. *Building Structure, 38,* 127–130.
Zhu, Y., & Cescotto, S. (1995). A fully coupled elasto-visco-plastic damage theory for anisotropic materials. *International Journal of Solids and Structures, 32,* 1607–1641.

Publisher's Note

Springer Nature remains neutral with regard to jurisdictional claims in published maps and institutional affiliations.